

DOT/FAA/AR-99/6

Office of Aviation Research
Washington, D.C. 20591

Fiber-Reinforced Structures for Turbine Engine Rotor Fragment Containment

September 1999

Final Report

This document is available to the U.S. public
through the National Technical Information
Service (NTIS), Springfield, Virginia 22161.



U.S. Department of Transportation
Federal Aviation Administration

DTIC QUALITY INSPECTED 4

19991109 108

NOTICE

This document is disseminated under the sponsorship of the U.S. Department of Transportation in the interest of information exchange. The United States Government assumes no liability for the contents or use thereof. The United States Government does not endorse products or manufacturers. Trade or manufacturer's names appear herein solely because they are considered essential to the objective of this report.

This report is available at the Federal Aviation Administration William J. Hughes Technical Center's Full-Text Technical Reports page: www.tc.faa.gov/its/act141/reportpage.html in Adobe Acrobat portable document format (PDF).

Technical Report Documentation Page

1. Report No. DOT/FAA/AR-99/6	2. Government Accession No.	3. Recipient's Catalog No.	
4. Title and Subtitle FIBER-REINFORCED STRUCTURES FOR TURBINE ENGINE ROTOR FRAGMENT CONTAINMENT		5. Report Date September 1999	
		6. Performing Organization Code	
7. Author(s) John Pepin	8. Performing Organization Report No.		
9. Performing Organization Name and Address Pepin Associates, Inc. North Main St. PO Box 397 Greenville, ME 04441		10. Work Unit No. (TRAIS)	
		11. Contract or Grant No. SBIR Phase II Contract DTRS-57-90-C-00025 MOD 4	
12. Sponsoring Agency Name and Address U.S. Department of Transportation Federal Aviation Administration Office of Aviation Research Washington, D.C. 20591		13. Type of Report and Period Covered Final Report	
		14. Sponsoring Agency Code ANE-100, ANM-100	
15. Supplementary Notes The FAA William J. Hughes Technical Center manager was William Emmerling.			
16. Abstract This program developed the designs for lightweight, fiber-reinforced structures to contain turbine engine rotor failures. These containment ring designs were based on a hybrid sandwich panel concept whose core consisted of several plies of a dry, ballistic fabric laminate. The structure of the panel consisted of metal facesheets mechanically connected with many small-diameter rods penetrating through the thickness of the fabric core laminate. This concept was developed by testing containment rings against a fixed energy level provided by the tri-hub disk burst of a T-53 power turbine stage. Ten spin tests were performed and the ring designs were varied to obtain the lightest-weight ring which would contain the rotor burst. Facesheet and rod structural elements were fabricated from either aluminum or titanium and candidate core materials were S glass, Kevlar®, and Zylon® (PBO). The Kevlar and Zylon organic fabrics performed well even at elevated temperature while the S glass was not very effective. Finally, a Kevlar/titanium containment ring design developed during the program was tested on a full-scale T-53 engine. The containment ring stopped the three disk fragments as they began to penetrate the engine case wall. This program resulted in containment ring and hybrid structure designs which can be used in either existing or new installations to satisfy specific containment requirements for certification.			
17. Key Words Uncontained turbine engine failure, Kevlar, Polybenzobisoxazole, Containment ring, Spin pit testing, Tri-hub failure, Rotor disc burst	18. Distribution Statement This document is available to the public through the National Technical Information Service (NTIS) Springfield, Virginia 22161.		
19. Security Classif. (of this report) Unclassified	20. Security Classif. (of this page) Unclassified	21. No. of Pages 49	22. Price

ACKNOWLEDGEMENTS

The FAA William J. Hughes Technical Center, Atlantic City International Airport, New Jersey, and Pepin Associates Inc., would like to thank the agencies that assisted and significantly contributed to the success of this test program. These agencies include the Naval Air Warfare Center, Aircraft Division, Trenton, New Jersey; Corpus Christi Army Depot, Corpus Christi, Texas; the New Jersey Army National Guard, Trenton, New Jersey; and the Naval Air Warfare Center, Weapons Division, China Lake, California.

TABLE OF CONTENTS

	Page
EXECUTIVE SUMMARY	ix
1. INTRODUCTION	1
1.1 Program Overview	1
1.2 Background on Turbine Rotor Fragment Containment	2
2. PROGRAM RESULTS	2
2.1 Examination of Materials	2
2.2 The Test Program	4
2.2.1 Test Program Objectives and Procedure	4
2.2.2 S Glass Containment Rings	7
2.2.3 Kevlar 29 Containment Rings, Small Diameter	11
2.2.4 Large-Diameter Kevlar 29 Containment Rings	18
2.2.5 Two Thermal Degradation Test Rings—Kevlar 29 and PBO	23
2.2.6 Full-Scale Trihub Burst Test of Containment Ring on the T-53 Engine	31
3. CONCLUSIONS	39
4. REFERENCES	40

LIST OF FIGURES

Figure	Page
1 Hybrid Structural/Energy-Absorbing Panel	1
2 Tensile Strength Retention After Thermal Treatment in Air of the PBO Fiber	4
3 Rotor Spin Facility at the Naval Air Warfare Center-Aircraft Division	6
4 Baseline S Glass Ring Made of a [0/90] S Glass Fabric Wrap With Teflon Interleaves	7
5 Posttest Photo of the Coated S Glass Ring	9
6 S Glass Ring With $\pm 45^\circ$ Reinforcement	10
7 Posttest Photo of S Glass Ring With $\pm 45^\circ$ Reinforcement	10
8 Layup of Baseline Kevlar Ring Which Forms the Energy-Absorbing Core of the Hybrid Sandwich Panel Design	12
9 Prepunched Facesheets Placed Around the OD and ID Surfaces	12
10 Ring Shown After Rods Have Been Inserted Through the Facesheets and Core	13
11 Baseline Kevlar Core Ring With Aluminum Structure Complete and Ready for Testing	13
12 Drawing of Baseline Small-Diameter Kevlar Ring Showing Dimensions	14
13 Baseline Kevlar Core Ring Installed in the Spin Chamber	14
14 Posttest Photo of Baseline Kevlar-Cored Hybrid Ring	15
15 High-Speed Photos of the Baseline Kevlar-Cored Aluminum Hybrid Ring During Test	16
16 Second Baseline Kevlar/Aluminum Hybrid Ring Mounted in the Spin Test Chamber	17
17 Posttest Photo of Second Baseline Kevlar/Aluminum Hybrid Ring	18
18 High-Speed Photos of First Large-Diameter Kevlar Containment Ring Spin Test With Combustor Case of T-53 Installed in Chamber	19
19 Close-Up Photo of Area Between Combustor Case and Containment Ring After Test of First Large-Diameter Kevlar Containment Ring	20

20	Thirty-Ply Kevlar Containment Ring With Aluminum Rods	20
21	Thirty-Ply Kevlar Containment Ring After Test; Close-Up View in Chamber	21
22	Thirty-Ply Kevlar Containment Ring After Test; Distant View in Chamber	21
23	Thirty-Ply Kevlar Containment Ring After Test; Combustor Case Placed Back Inside Ring	22
24	Pretest Photo of the Large-Diameter 30-Ply Kevlar Ring Tested Without the Engine Combustor Case	22
25	Posttest Photo of the Large-Diameter 30-Ply Kevlar Containment Ring Tested Without the Engine Combustor Case	23
26	Kevlar Thermal Test Ring Before Temperature Exposure	24
27	Kevlar Thermal Test Ring Mounted to Chamber Cover Ready for Testing	25
28	Posttest Photo of Kevlar Thermal Test Ring	25
29	Oven Used to Heat the Thermal Test Rings Just Before Spin Testing	26
30	Cutting the PBO Fabric at a 45° Angle	27
31	Close-Up of Manual Cutting of PBO Fabric	27
32	Sewing Draw String Strips to Edge of Fabric	28
33	Layup of PBO Containment Ring	28
34	Finished PBO Containment Ring	29
35	PBO Containment Ring Suspended From Cover of Spin Chamber	29
36	Posttest Photo Showing PBO Ring, Fragments, and Heating Elements	30
37	Close-Up of PBO Ring After Testing	31
38	ID Grinding Operation	32
39	Grinding Rod Ends on ID Surface of Full-Scale Test Containment Ring	33
40	Laser Setup for Welding ID Surface of Full-Scale Test Containment Ring	33
41	Completed Full-Scale Test Containment Ring	34
42	T-53 Engine Used in Full-Scale Test	35

43	View From the Aft End of the T-53 Engine Showing the Second Stage Power Turbine	35
44	Full-Scale Test Setup Showing T-53 Engine and Containment Ring Before Test	36
45	Posttest Photo Showing Helicopter Airframe, Engine, and Containment Ring	37
46	Close-Up of the Left Side of the Engine Shows Outer Facesheet Peeled Back	37
47	View From Tailpipe; Bulges in the Ring Indicate Disk Fragment Impact	38
48	Posttest View From the Right Side of the Engine	38

LIST OF TABLES

Table		Page
1	Properties of Fibers	3
2	Effect of Time at Temperature on Tensile Strength of Kevlar 29	4
3	Containment Ring Design and Test Summary	39

EXECUTIVE SUMMARY

This program was an extension of work previously performed to develop fiber-reinforced structures for turbine engine rotor fragment containment. In the previous program a hybrid sandwich panel concept was shown to be effective as both a static structure member and as a containment barrier to protect critical aircraft systems from high-energy fragments. This concept is a sandwich panel whose core consists of dry, energy-absorbing fabric layers. The dry core laminate is penetrated through its thickness by many closed spaced rigid rods which are attached to the panel's facesheets. Using this concept containment rings were fabricated and tested to develop lightweight designs capable of containing a tri-hub disk burst.

Two material types are needed for the sandwich panel design—a ballistic energy-absorbing fabric and a lightweight structural material. Materials selected for testing here included Kevlar 29, PBO (polybenzobisoxazole), and S glass fibers for the core and aluminum and titanium for the facesheets and rods. Ten spin chamber tests were performed to develop the containment ring designs. Spin testing was performed using a T-53 second stage power turbine which was modified to fail in a tri-hub disk burst mode. This testing was done at the Naval Air Warfare Center Rotor Spin Facility in Trenton, New Jersey. Although the dry S glass was not very effective, testing showed good baseline performance by Kevlar 29 and very strong potential for PBO, both at room temperature and after aging at 200°C for 500 hours.

Using the spin test results, an additional ring was fabricated for a full-scale test in which a T-53 engine mounted on a helicopter airframe was modified to fail in a tri-hub disk burst mode. This full-scale test containment ring had a Kevlar 29 fabric core and titanium structural rods and facesheets. This ring successfully contained the engine failure.

The program results describe containment structure design characteristics to stop rotor disk bursts and these results can guide engine and airframe structure design to minimize the weight/space penalty for containment of turbine engine failures.

1. INTRODUCTION.

1.1 PROGRAM OVERVIEW.

This program was built upon previous work [1] to develop lightweight fiber-reinforced structures to contain turbine engine rotor failures. In this previous program a hybrid sandwich panel concept was shown to be effective as both a static structure member and as a containment barrier to protect critical aircraft systems from high-energy fragments. This concept is a sandwich panel whose core consists of dry, energy-absorbing fabric layers. This dry laminate is penetrated through its thickness by many closely spaced rigid rods which are attached to the panel's facesheets. These rods mechanically connect the facesheets as would a honeycomb core such that the panel can support shear, compressive, and tensile loads. Figure 1 shows a drawing of this panel.

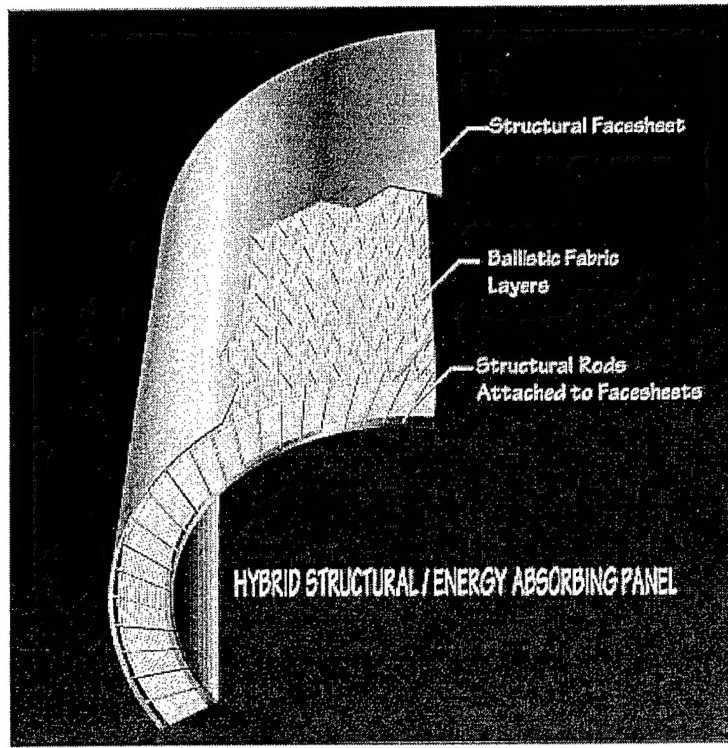


FIGURE 1. HYBRID STRUCTURAL/ENERGY-ABSORBING PANEL

In the previous program the structural material used was graphite/epoxy while the energy-absorbing materials tested included Kevlar 29 and PBO (polybenzobisoxazole). Both the [0/90] and the $\pm 45^\circ$ fiber-reinforcement orientations of the energy-absorbing fabric were tested showing the weight advantage of the off-axis design. It was also shown that PBO fiber has good potential as a material for containment structures due to its high specific strength, toughness, and good temperature stability. The work presented here extended the previous work in the following ways:

- a. Examined S Glass as a potential high-temperature containment material.

- b. Performed spin tests of PBO and Kevlar at elevated temperature.
- c. Expanded testing on the $\pm 45^\circ$ fiber-reinforcement architecture in Kevlar, S Glass, and PBO.
- d. Better simulated the T-53 disk failure event by placing engine structure in the spin chamber.
- e. Developed a technique to fabricate a hybrid containment ring with a metal structure.
- f. Fabricated and tested a hybrid titanium/Kevlar containment ring on a full-scale T-53 engine.

Ten developmental containment rings were fabricated and spin tested. Spin testing was performed using a T-53 engine second stage power turbine which was modified to fail in a tri-hub disk burst mode. This testing was done in the Naval Air Warfare Center Rotor Spin Facility in Trenton, New Jersey. The ten containment rings included S glass, Kevlar, and PBO of various designs. In addition to the ten spin tests, one full-scale test was performed to demonstrate the containment of a tri-hub disk burst failure on a running T-53 engine. The containment ring for this test was composed of a Kevlar fabric core with through-the-thickness rods and facesheets of titanium. Unique laser welding techniques were developed to weld the facesheet/rod joints in close proximity to the underlying organic fiber fabrics. The results of this program are presented in section 2.0 and show the potential of the hybrid panel concept in combination with PBO and Kevlar fabrics to provide lightweight containment systems for turbine engines.

1.2 BACKGROUND ON TURBINE ROTOR FRAGMENT CONTAINMENT.

Since the advent of turbine-powered aircraft, the risk of turbine engine rotor failures and damage from resulting high-energy fragments have been present. Although uncontained rotor failures are thankfully rare, significant damage can result when these events do occur. In some cases high-energy rotor fragments have severed control cables, fuel lines, and other critical systems. Such fragments have also penetrated fuel tanks, pressurized fuselage skin and frames, and other engines on the aircraft. The Federal Aviation Administration (FAA) has established regulations and design guidelines for engine failures in Federal Aviation Regulation (FAR) 33 subpart B which defines engine design requirements and FARs 23 and 25 which include design precautions to minimize hazards from uncontained engine and auxiliary power unit (APU) failures. Advisory Circulars (AC) [2] also serve as design guidelines for the location of critical systems and components relative to the engine rotors and fan blades. Historical data on uncontained failures has been studied by the Society of Automotive Engineers [3].

2. PROGRAM RESULTS.

2.1 EXAMINATION OF MATERIALS.

The hybrid sandwich panel concept uses two material systems or types—a dry fabric laminate core to absorb high kinetic energy fragments and a structural material which forms the rods and facesheets giving the sandwich panel its stiffness and strength. Material candidates for the energy-absorbing fabric core can be selected from high-performance organic fibers used in

ballistic fabrics—aramid (Kevlar), polyethylene (Spectra), and the developmental fiber, polybenzobisoxazole (PBO). S glass has also been used in ballistic applications although its density is higher and its toughness is not equal to the organic fibers. Properties of these fibers are given in table 1. Materials for the structure of the panel can be metals or structural composites. In the previous program, graphite/epoxy was used but airframe manufacturers have indicated that a metal structure around the core would be of more interest from a maintainability and durability standpoint. Therefore, in the current program titanium and aluminum are used for the structural rods and facesheets.

TABLE 1. PROPERTIES OF FIBERS

	Kevlar 29	Dry PBO	PBO, Heat Treated	Spectra 1000	S Glass
Density, g/cc	1.44	1.50-1.56	1.50 - 1.56	0.97	2.5
Tensile strength, MPa	3600	5958	5958	2830	4585
Tensile modulus, GPa	83	172.1-198.6	238.3 - 251.6	103	88.9
Tensile elongation, %	4	3.5-4	1.5	3.1	5.7

Kevlar has been the standard material for lightweight containment over the years. It has reasonably high strength and toughness and is often used in fan cases. Its strength, however, is reduced after exposure to elevated temperature as shown in table 2. PBO is a developmental fiber whose manufacturing rights have been transferred from Dow to Toyobo. Toyobo began to sell this fiber commercially under the trade name Zylon™ in late 1998. The properties of PBO show its potential both as a ballistic energy-absorbing material as well as a reinforcement for structural composites. PBO is less hygroscopic than Kevlar so keeping moisture out of a dry or impregnated laminate is not as difficult. PBO has good retained strength at 200°C for 1000 hours as shown in figure 2 [4] but NASA investigators [5] have found that long term thermal aging of PBO at 204°C for three and six months significantly reduced its tensile strength. The same NASA study did find, however, that PBO in the “as received” condition was significantly better in ballistic tests than Kevlar at both room temperature and 260°C. More work is needed to determine the time/temperature limits of the production version of PBO. Pepin Associates, Toyobo, and NASA Lewis are planning a long-term aging study to 10,000 hours for PBO and Kevlar 29. Both PBO and Kevlar 29 are used to fabricate test containment rings in this program.

As mentioned above, S glass is a candidate for containment structures because of its high strength and temperature resistance. Since the glass filament strength is a strong function of its surface imperfections, glass is most often used in resin matrix laminates when ballistic protection is the goal. When the filament is encased in a resin, the surface is protected and the laminate's ability to absorb energy is enhanced. For use in the hybrid sandwich panel, however, the glass fabric would be dry to save weight and enhance the temperature capability of the sandwich panel structure since no organic resin would be involved. The test program includes dry S glass fabric rings to test the efficiency of the dry glass fabric to absorb the fragment energies.

TABLE 2. EFFECT OF TIME AT TEMPERATURE ON TENSILE STRENGTH OF KEVLAR 29

Tensile Strength	Time at Temperature
2896 MPa (420 ksi)	0 hrs @ room temp
2620 MPa (380 ksi)	500 hrs @ 160°C
1103 MPa (160 ksi)	500 hrs @ 200°C
1467 MPa (210 ksi)	300 hrs @ 200°C
1724 MPa (250 ksi)	200 hrs @ 200°C
2206 MPa (320 ksi)	100 hrs @ 200°C

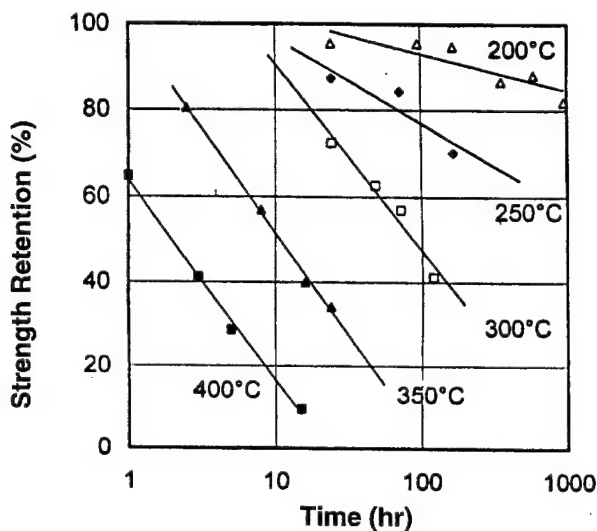


FIGURE 2. TENSILE STRENGTH RETENTION AFTER THERMAL TREATMENT IN AIR OF THE PBO FIBER

Spectra has some weight advantage over Kevlar especially for very high velocities. Allied Signal estimates that for the standard threat of 0.23 kg at 152 m/sec, Spectra would be 20% lighter but 30% more costly than Kevlar. This has not been demonstrated, however. Some drawbacks of Spectra for containment applications include its flammability and a sharp drop in properties above 100°C. Flammability is being addressed with intumescent coatings and mixing the Spectra with glass. Spectra is being considered for baggage container hardening but, due to its temperature limitations, it was not included in the current test program for containment.

2.2 THE TEST PROGRAM.

2.2.1 Test Program Objectives and Procedure.

The goal of the test program was to determine the lightest-weight containment ring design which would contain a 113,000 Joule tri-hub rotor burst. To achieve this objective a series of ten spin tests were performed in an iterative fashion. For a given material, a containment ring

architecture and design were selected and the ring was built and spin tested. Using the results of this test an improved containment ring was designed and tested. This process was repeated in an iterative fashion to seek a threshold design for containment—that is, if the design were made any lighter by removing plies of fabric and the like, then the ring would not fully contain the rotor burst.

The spin testing was performed at the Naval Air Warfare Center in Trenton, New Jersey. Figure 3 shows a schematic of the chamber and associated hardware required to perform the test. The test rotor was mounted inside the chamber to a shaft which penetrates vertically through the chamber's top cover. The rotor was driven by an air-drive turbine attached to the outside of the top cover. The containment ring was suspended from the cover and surrounds the rotor such that the rotor's disk plane coincided with the horizontal midplane of the containment ring. A thin, aluminum sheet witness ring was also attached to the cover and surrounded the containment structure some distance away. Its purpose was to record fragment penetration of the containment structure. Fragments which could penetrate the structure would also penetrate or, if at small energies, dent the witness ring. The chamber was evacuated to approximately 8-mm Hg to reduce aerodynamic forces on the rotor allowing the air turbine to quickly accelerate the rotor to its burst speed. The rotor disk was partially cut radially inward in three places 120° apart such that the disk would fail in a tri-hub burst mode upon reaching a predetermined rotational speed.

The rotor used in these tests was a T-53 engine Model 13, second stage power turbine, and it was modified to fail at 20,400 rpm giving a burst kinetic energy of 113,000 Joules.

A Cordin high-speed camera recorded the impact event by viewing through a port at the side of the chamber and a 45° mirror inside which allowed a view up at the rotor. The repeating electronic flash which actually causes these pictures to be taken was initiated by signal interruption from a trigger strip bonded around the inside of the containment structure. This signal interruption also fixed the time at which the rotor speed was recorded. The nominal camera framing rate is 13000 frames/sec and about 40 pictures are taken during the event.

Following the ten spin tests, a full-scale engine test was performed at the Naval Air Warfare Center, Weapon Division at China Lake, California (NAWCWD-China Lake). This test was done to verify that the containment ring designs developed with the spin tests could in fact stop the disk fragments from a failed turbine disk on a full-scale engine. The T-53 engine was mounted on a helicopter airframe and run until the turbine rotor rpm reached the same critical speed as that used in the spin testing. Modification of the turbine rotor to fail in this fashion was performed by NAWCAD-TRN. The rotor modification was the same as used for the spin tests except that the turbine shaft itself was also weakened by cutting a circumferential groove in the shaft leaving a radial thickness of 3.2 mm in the shaft. This modification was verified by spin testing at the Trenton Navy facility. Both real-time and high-speed video were taken of this full-scale test.

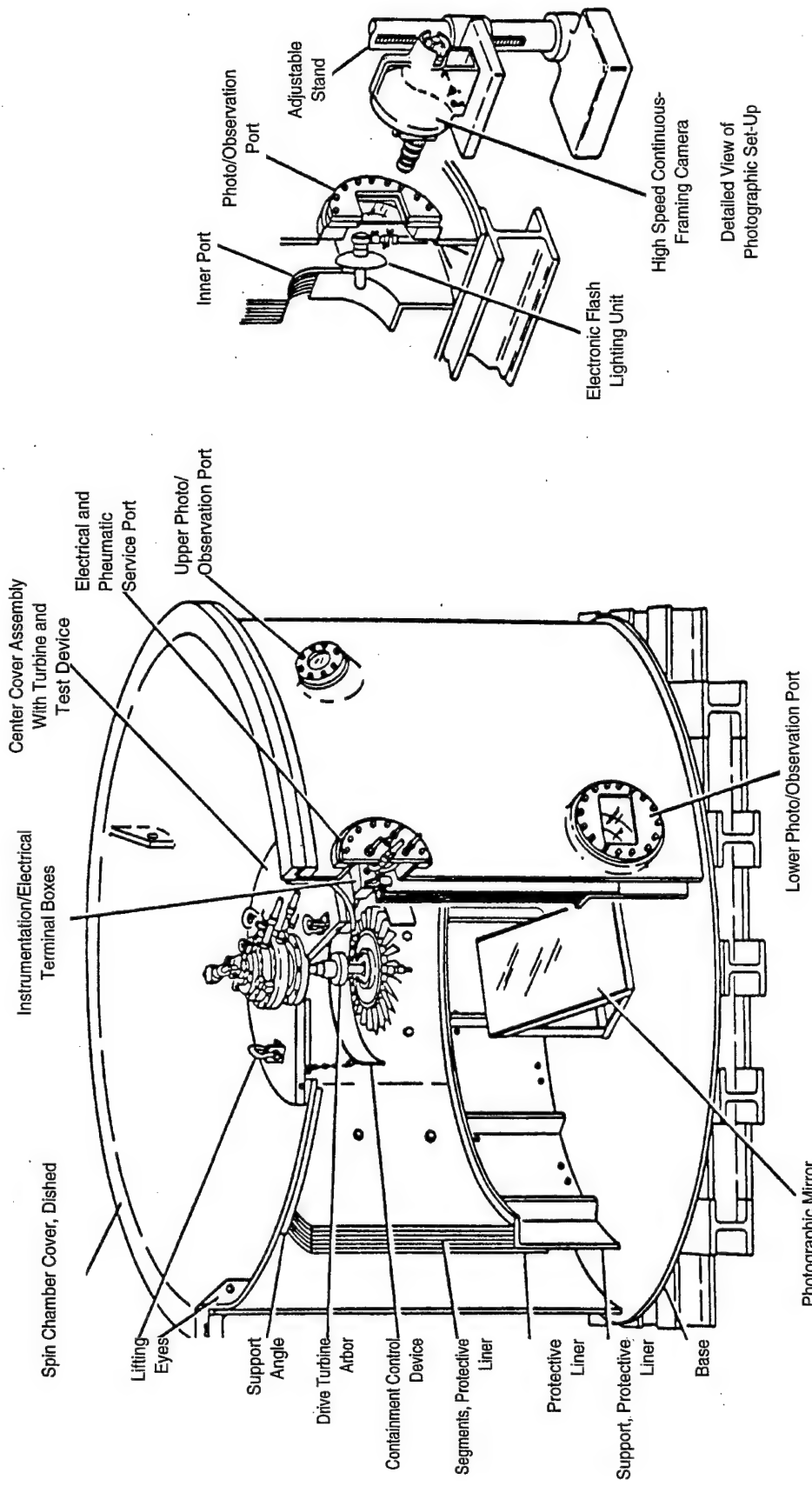


FIGURE 3. ROTOR SPIN FACILITY AT THE NAVAL AIR WARFARE CENTER-AIRCRAFT DIVISION

Individual ring designs, fabrication methods, and the results of the tests for each of the eleven containment rings are given in the following section.

2.2.2 S Glass Containment Rings.

S glass is a low-cost, high-strength fiber which is used to reinforce ballistic panels for ships, armored vehicles, and other applications. It is included here because of its potential as an intermediate temperature ballistic material. Three S glass containment rings were fabricated by wrapping glass fabric around an internal mandrel as in a jellyroll.

2.2.2.1 Baseline S Glass Containment Ring Design and Fabrication.

The baseline S glass containment ring was fabricated by wrapping a dry fabric around a 37.18-cm-diameter mandrel to form a multi-ply ring. The fabric was a [0/90] plain weave using 1250 yield S glass from Owens Corning. The fabric weave spacing was 9.4 x 9.4 cm and the fabric was wrapped such that the fiber reinforcement directions of the fabric were aligned with the axial and circumferential directions of the ring. Each ply of the fabric was interleaved with a 0.025-mm-thick Teflon film to reduce abrasion between plies of the glass during the impact. The total number of plies was 38.5 and the ring had a mass of 9.64 kg (21.25 lbs). The ring axial length was 25 cm and this dimension is common to all the test rings. The top and bottom edges of the ring were sewn with Kevlar thread to increase the ring's rigidity. Figure 4 shows this completed ring surrounding the T-53 rotor.

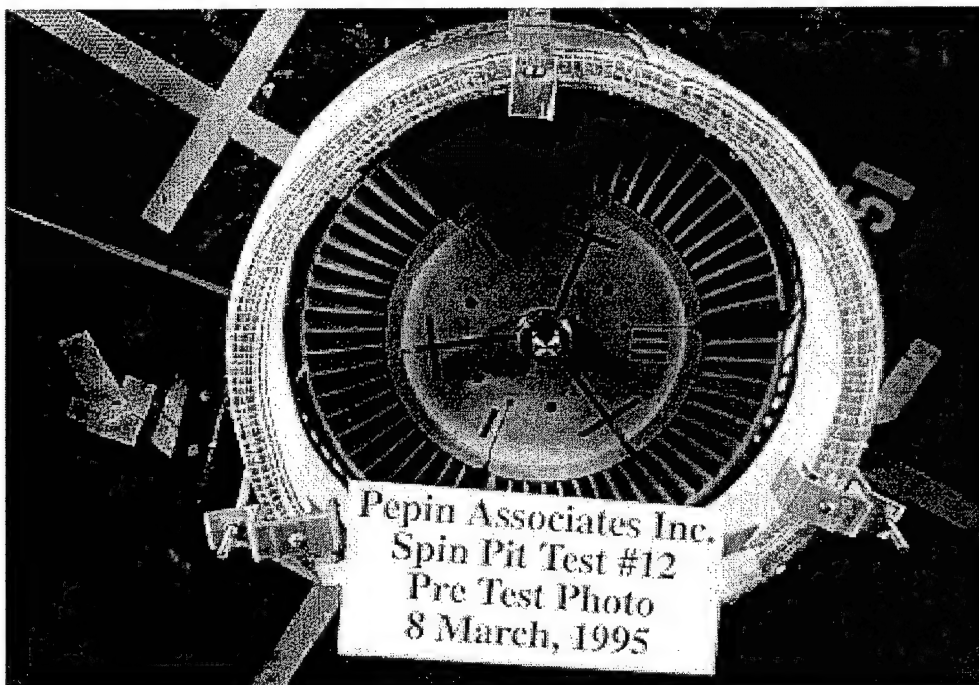


FIGURE 4. BASELINE S GLASS RING MADE OF A [0/90] S GLASS FABRIC WRAP WITH TEFLON INTERLEAVES

2.2.2.2 Test Results for Baseline S Glass Containment Ring.

The spin test was performed on the S glass ring and all three disk fragments penetrated through it. The witness ring showed the three large holes made by the disk fragments as well as smaller holes made by blade fragments. These blade fragments escaped through the large disk segment holes in the containment ring. Other blade fragments penetrated through 8-10 plies of the containment ring before being trapped in the glass fabric.

2.2.2.3 Polyimide Coated S Glass Containment Ring Design and Fabrication.

The next ring design once again used S glass but the glass fibers were coated with a polyimide resin to try to protect them against abrasion. This resin was applied as an aqueous solution of DuPont's polyamic acid/imide with 6% resin solids and then baked in air at 200°C for 13 hrs. The baking converts the applied solution to a polyimide which coats the filament surface.

The fabrication method was the same as for the baseline ring. Fifty-three layers of [0/90] S glass fabric were wrapped around the mandrel. The resin was added as the ring was wrapped, and the fully wrapped ring was heat treated to cure the resin. The fabric was a 8.3- x 8.3-cm plain weave woven from Owens Corning 1250 yield S glass with a 449AA sizing. Finished ring mass was 13.6 kg (30 lbs). Inside diameter was 36.9 cm while the axial length was 26.9 cm, a little larger than the nominal 22.9 cm.

2.2.2.4 Coated S Glass Ring Test Results.

The test was successfully run. Two disk fragments were contained within the ring while one penetrated through the ring. Blade fragments also escaped through the hole made by the disk fragment. One hole in the witness ring, about 10.16 cm long, was probably the result of a broken air-drive turbine shaft fragment upon failure. Figure 5 is a posttest photo of this ring showing the hole made by the disk fragment which escaped.

2.2.2.5 S Glass Containment Ring With 45° Reinforcement: Design and Fabrication.

The next S glass ring used glass fabric plies cut at a 45° angle so that the reinforcement in the ring wall was at ±45° to the ring axis. This design has worked well in the past for Kevlar rings but it has never been tried with glass. The off-axis reinforcement allows the ring wall to easily expand radially providing a greater distance over which to stop the impacting fragments. The fabric used was an off-the-shelf plain weave S glass fabric from Hexcel. It used 250 yield roving resulting in a 2- x 2-cm weave. The plies were wrapped as before until 51 layers were built up on the mandrel.

In a previous test using the ±45° reinforcement, one of the disk fragments flipped out of the ring at a relatively low velocity. This S glass containment ring included draw strings at the ring edges to form a pocket to trap the disk fragments and prevent their escape. These were 5-cm-wide [0/90] strips sewn into the edges of six of the ±45° plies. The fabric used was a 7.9- x 7.9-cm plain weave S glass fabric. These six plies were evenly distributed through the thickness of



FIGURE 5. POSTTEST PHOTO OF THE COATED S GLASS RING

the ring and the entire edge was sewn through to bind it together. As the ring was impacted along its central plane by the disk fragments, the containment ring expanded radially, and the ring shrunk in height due to the fiber architecture. The edges of the ring, however, were more restricted in their ease of radial expansion because of the [0/90] strips. This created a pocket in the ring which prevented the disk fragments from flipping out of the stretched ring.

This ring's mass was 13.6 kg (30 lbs) with an axial length of 25.4 cm and an inner diameter (ID) of 36.9 cm. A photo of the ring is shown as figure 6.

2.2.2.6 Test Results for S Glass Containment Ring With $\pm 45^\circ$ Reinforcement.

The S Glass ring with $\pm 45^\circ$ reinforcement did not contain the rotor burst. One of the disk fragments penetrated the ring wall while the other two remained within the ring. Figure 7 is a posttest photo of this ring.



FIGURE 6. S GLASS RING WITH $\pm 45^\circ$ REINFORCEMENT

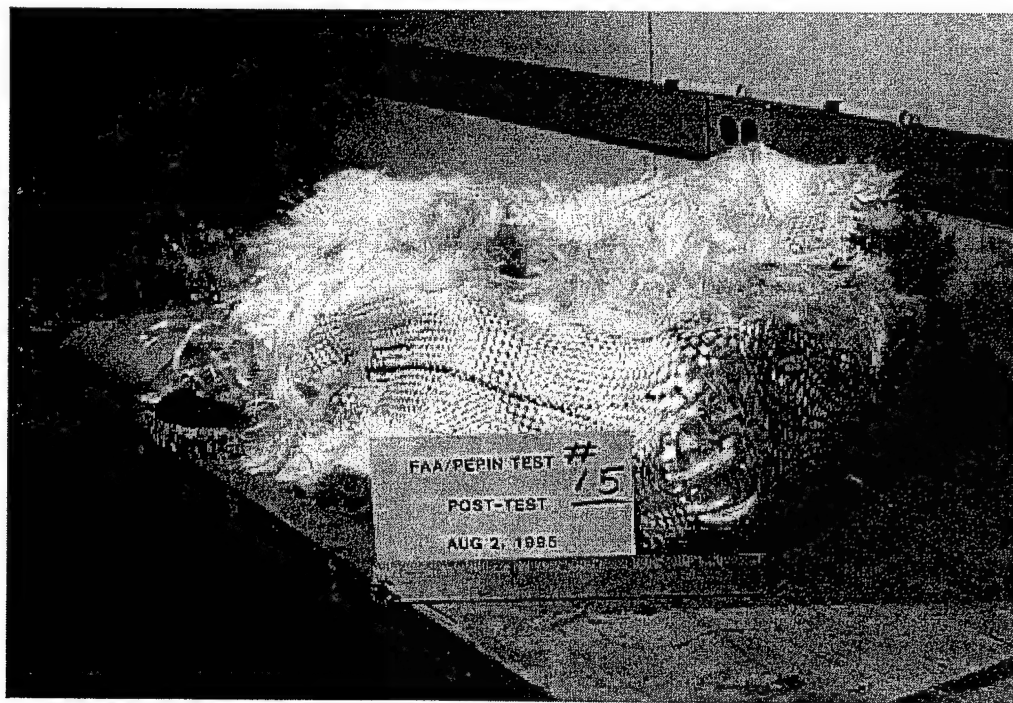


FIGURE 7. POSTTEST PHOTO OF S GLASS RING WITH $\pm 45^\circ$ REINFORCEMENT

2.2.2.7 Test Result Summary for Glass Rings.

The glass ring test results were quite poor. Ring masses in excess of 13 kg did not stop the rotor fragments and attempts to coat the fabric or use off-axis reinforcement designs did not significantly improve the performance of the glass to the point where it would be of interest for this containment application. However, dry, unimpregnated S glass used in reference 6 indicates that the [0/90] S glass performance is comparable to [0/90] Kevlar 29 and PBO performance.

2.2.3 Kevlar 29 Containment Rings, Small Diameter.

Kevlar 29 based containment rings were fabricated with the $\pm 45^\circ$ reinforcement architecture used in the previous glass ring and also in a previously tested Kevlar 29 ring. Again, this architecture allows large radial deformation and a lighter-weight ring to contain a given energy level. Both small-diameter and large-diameter Kevlar rings were fabricated. The small-diameter rings just fit around the rotor itself with 12-mm clearance between the rotor shroud and the ring inside wall. The glass rings were this size. The large-diameter rings were fabricated to fit around the T-53 engine outer case. This outer case structure was placed in the spin chamber to simulate more closely an actual engine failure. This section discusses the two small-diameter Kevlar ring results while the following section gives results for the large-diameter Kevlar rings.

2.2.3.1 Small-Diameter Kevlar Ring Baseline Design and Fabrication.

This ring was designed as a hybrid sandwich panel with a dry Kevlar fabric core and aluminum through-the-thickness rods and covering facesheets. It was made by first cutting 22.9-cm-wide strips of Kevlar 29 style 745 fabric at a 45° angle to the warp direction of a 152-cm-wide fabric. The strips were thus reinforced at $\pm 45^\circ$ to their longitudinal axis. They were then wrapped around a mandrel to form the ring's core. As the strips were added to the mandrel they were lightly sewn to the strips below to hold them in place and the joints were staggered throughout the layup. This ring also included draw strings at the ring edges as in the previous glass ring. These were the 5-cm-wide [0/90] strips sewn into the edges of six of the $\pm 45^\circ$ plies. These six plies were again evenly distributed through the thickness of the ring. The 42 layers of fabric had a wall thickness of 2.80 cm (1.1 in).

After the Kevlar layup had been fabricated and sewn into the ring shape, 5052 aluminum facesheets 0.812 mm thick with prepunched holes were wrapped around the inside and outside diameters of the ring and held in place with tie wraps at the outer diameter (OD) and steel rings at the ID. Aluminum rods, 1.57 mm in diameter, were then inserted manually through holes in the facesheets. These rods were also 5052 aluminum and were inserted at + and - 45° to the facesheets alternating between one circumferential row and the next. The rods were then cut to allow them to just protrude above the facesheets, and these joints were then tungsten-inert-gas (TIG) welded. Aluminum endcap sheets were then welded into place to cover the ends of the ring. The total mass of the ring was 7.14 kg while the mass of the Kevlar alone was 5.39 kg. Figures 8 through 10 show the sequence of manufacturing steps. The finished ring is shown in figure 11. Figure 12 shows a drawing of the ring and figure 13 shows the ring installed in the spin chamber.

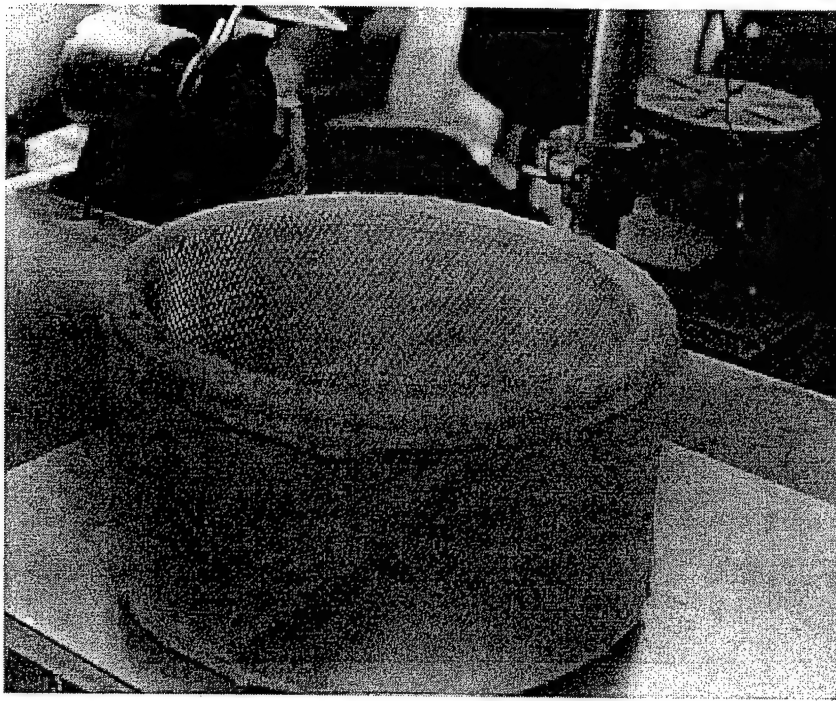


FIGURE 8. LAYUP OF BASELINE KEVLAR RING WHICH FORMS THE ENERGY-ABSORBING CORE OF THE HYBRID SANDWICH PANEL DESIGN

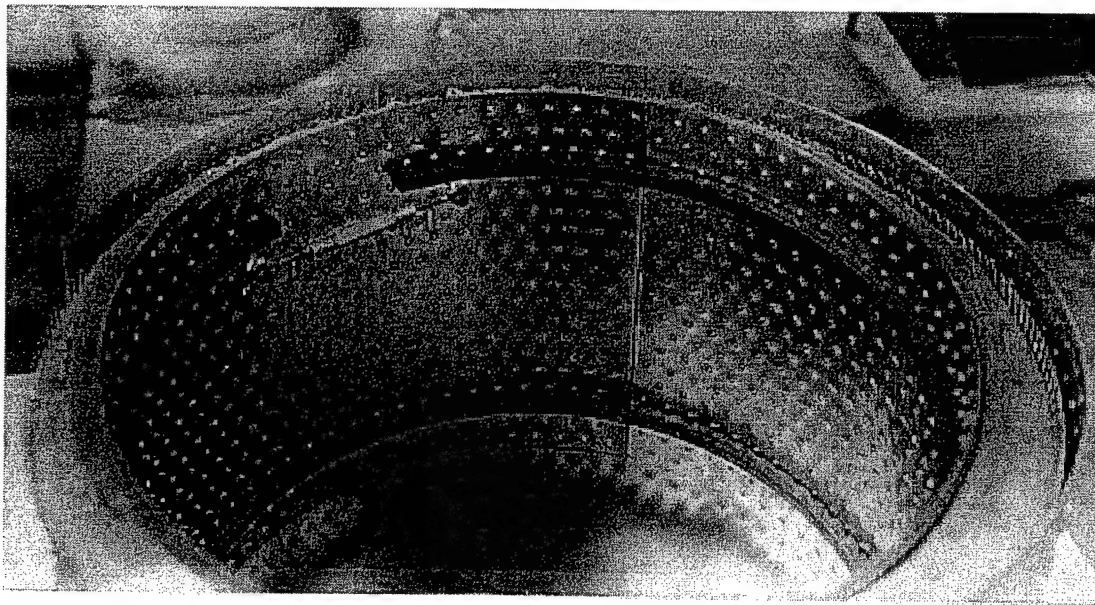


FIGURE 9. PREPUNCHED FACESHEETS PLACED AROUND THE OD AND ID SURFACES

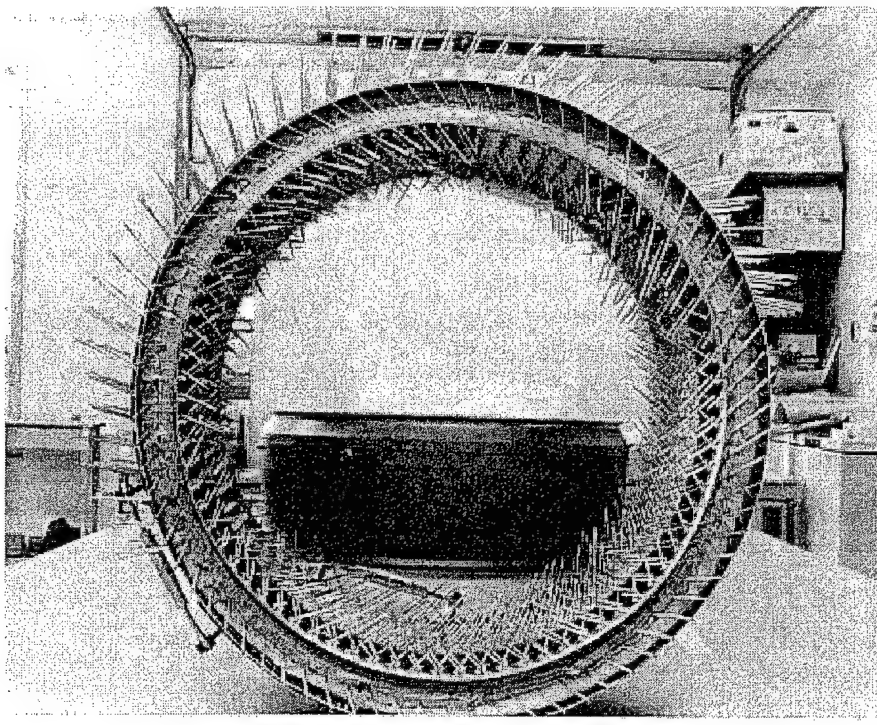


FIGURE 10. RING SHOWN AFTER RODS HAVE BEEN INSERTED THROUGH THE FACESHEETS AND CORE

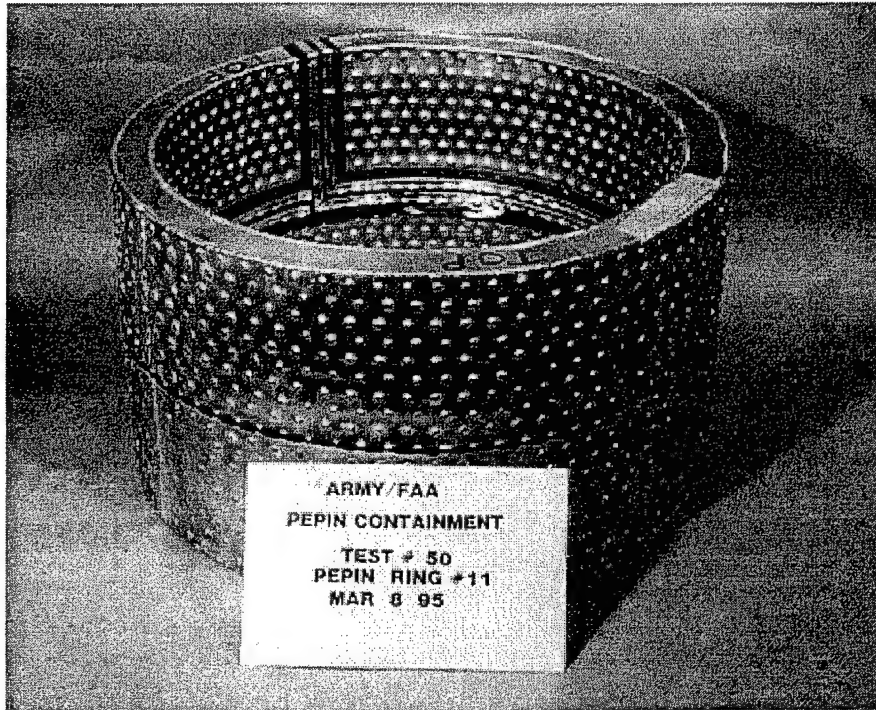


FIGURE 11. BASELINE KEVLAR CORE RING WITH ALUMINUM STRUCTURE COMPLETE AND READY FOR TESTING

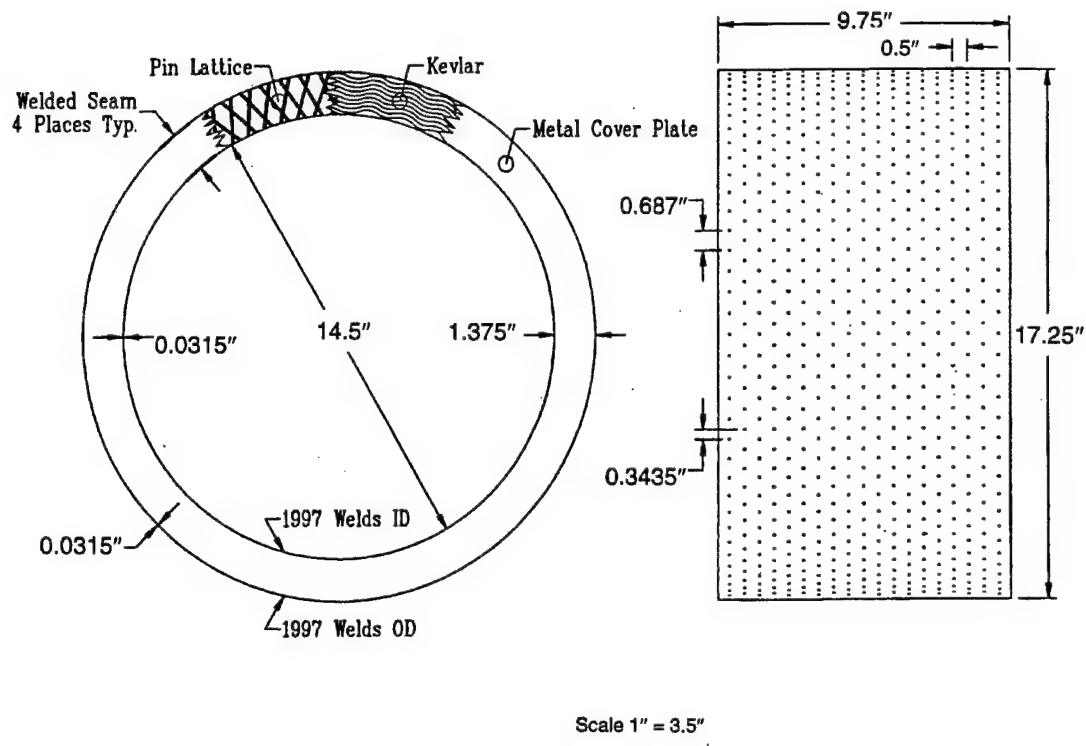


FIGURE 12. DRAWING OF BASELINE SMALL-DIAMETER KEVLAR RING SHOWING DIMENSIONS

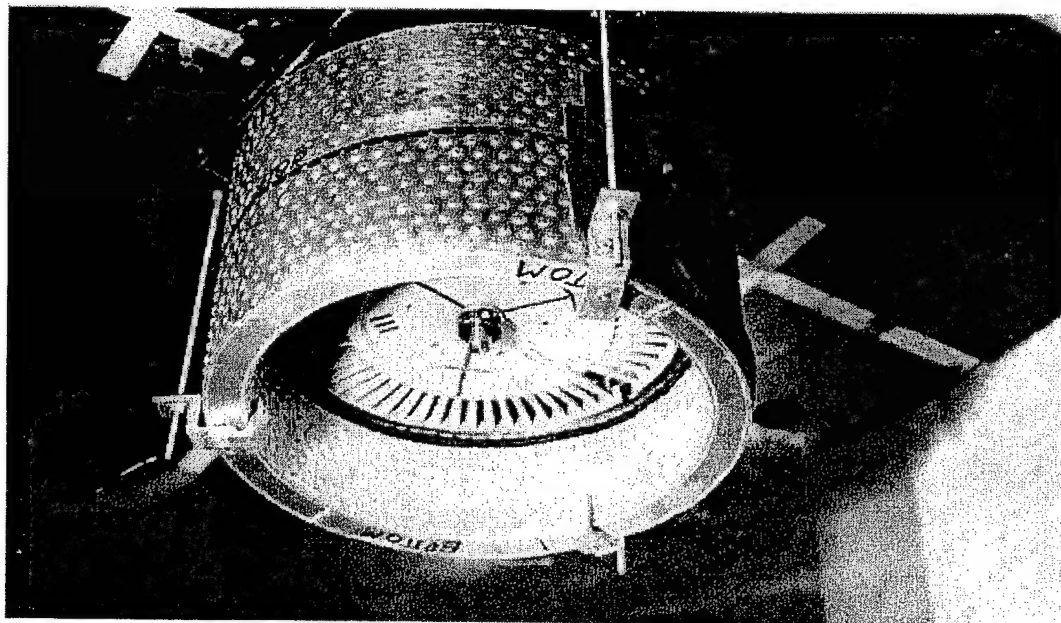


FIGURE 13. BASELINE KEVLAR CORE RING INSTALLED IN THE SPIN CHAMBER

2.2.3.2 Test Results for Baseline Kevlar-Cored Hybrid Ring.

The T-53 rotor failed at 20,800 rpm, but one of the disk fragments broke up into several smaller pieces. Even though all of the fragments were contained, the test was invalid because of the breakup of one of the disk segments. The trihub burst is the most severe containment condition and the one to which all of the other containment structures are compared. This test therefore had to be repeated. A posttest photo is shown in figure 14. The high-speed photos of figure 15 depict the event at the various time steps shown. Note the breakup of one of the disk fragments and the deformation of the containment ring as the disk fragments impact.

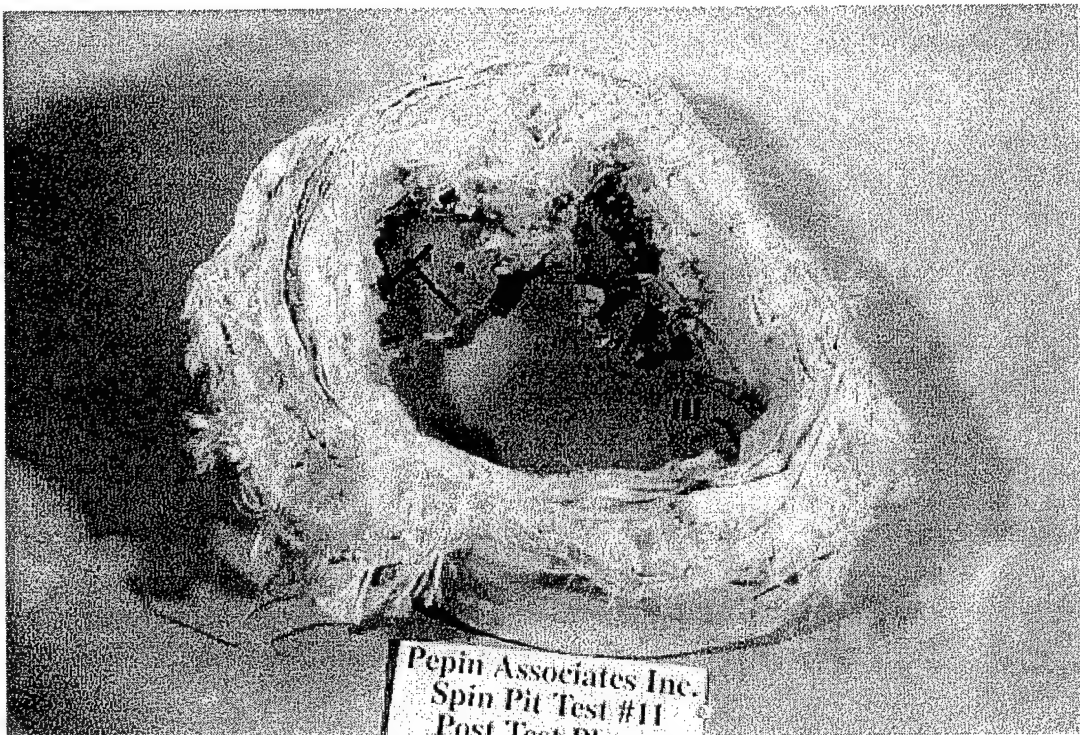
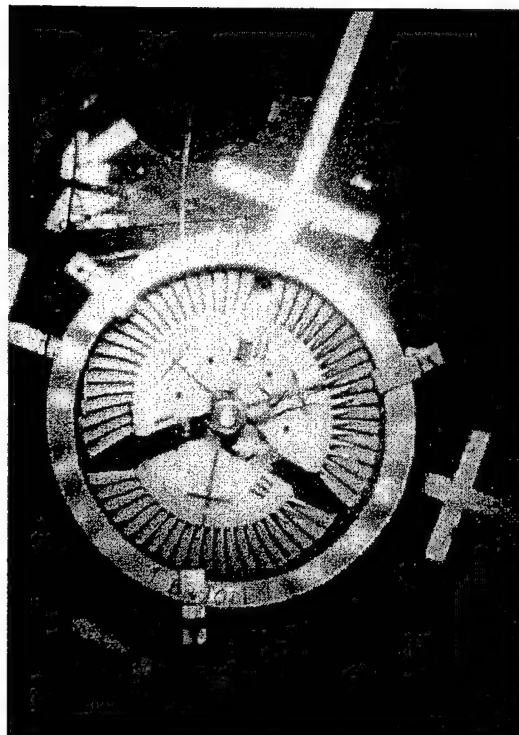


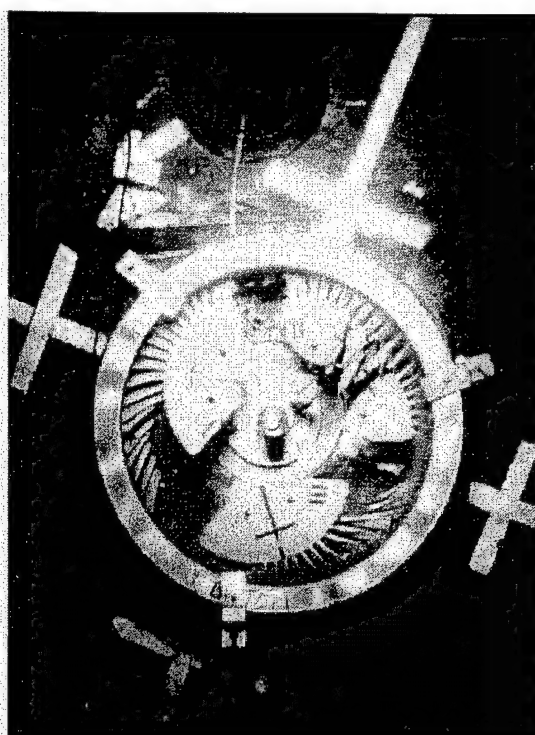
FIGURE 14. POSTTEST PHOTO OF BASELINE KEVLAR-CORED HYBRID RING

2.2.3.3 Baseline Kevlar Ring 2 Fabricated for Retest.

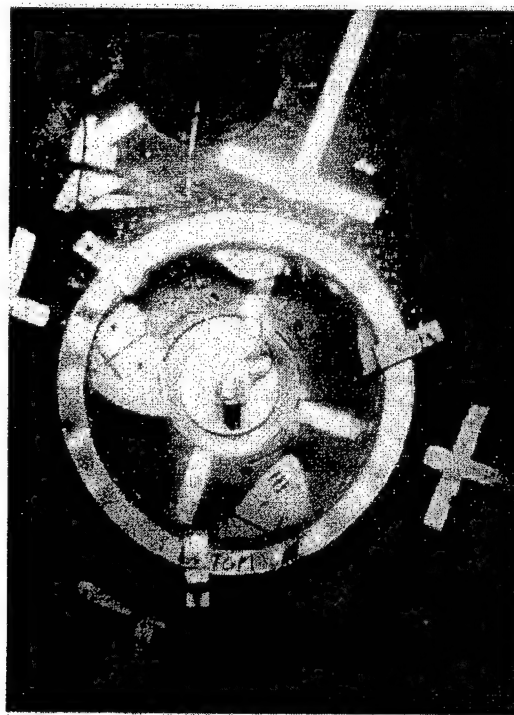
The second baseline ring was fabricated with essentially the same design as the first. Kevlar style 745 fabric strips with $\pm 45^\circ$ orientation were wrapped onto the mandrel and lightly sewn into place. Hoop reinforcement on the edges of these plies was added every seventh ply. This reinforcement consisted of a 5-cm-wide strip of [0/90] Kevlar fabric sewn to the edges of the primary $\pm 45^\circ$ plies. Again this hoop reinforcement acts as a draw string on the edges to trap the disk fragments in the ring. After 43 plies were wrapped onto the mandrel and the edges were sewn to give the fabric layup some stability, the aluminum rods were inserted through the fabric ring's thickness in the same array as for the first baseline ring. In this case, however, the rods were inserted by a manually operated machine which saved a great deal of time over the previous all manual method.



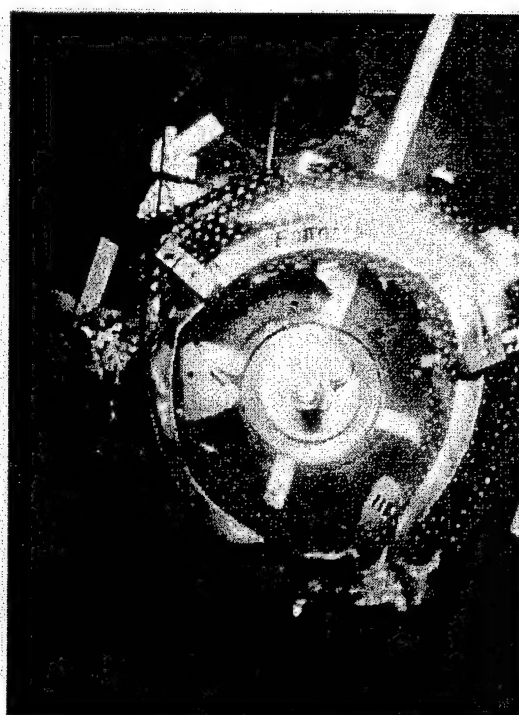
time = 0 msec



$t = 0.46$ msec



$t = 0.92$ msec



$t = 2.1$ msec

FIGURE 15. HIGH-SPEED PHOTOS OF THE BASELINE KEVLAR-CORED ALUMINUM HYBRID RING DURING TEST

Aluminum facesheets were then wrapped to touch the exposed rod ends on both the ID and OD surfaces. These facesheets were held in place by injecting urethane foam in the annular region between the facesheet surface and the fabric surface. The foam flowed around the exposed rods and, upon curing, bonded the facesheets to the ring. This was not a structural bond but merely demonstrated a concept for possible future attachment of the facesheets with a stronger foam or other injectable material. This method of facesheet attachment would not materially affect the test outcome since the containment ability of the ring is dominated by the ballistic fabric core design. This second baseline ring is shown suspended from the cover in the spin chamber in figure 16. The mass of this ring was 8.81 kg and the mass of the Kevlar core was 6.84 kg.

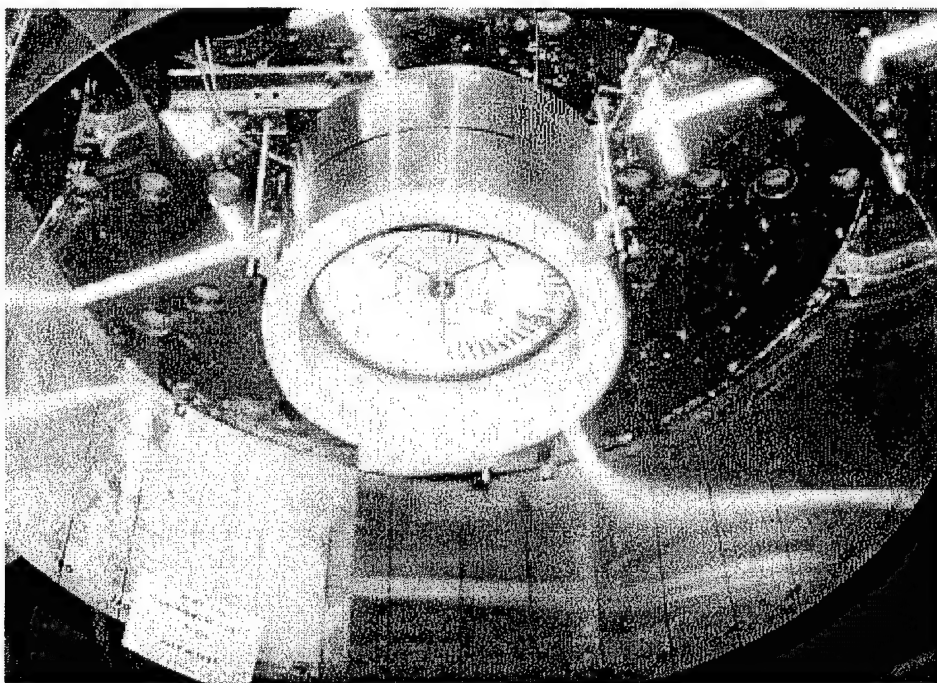


FIGURE 16. SECOND BASELINE KEVLAR/ALUMINUM HYBRID RING MOUNTED IN THE SPIN TEST CHAMBER

2.2.3.4 Second Baseline Kevlar Ring Test Results.

This second baseline ring contained all fragments released from the rotor. The three disk fragments were found in the ring itself following the test. All the rods remained in the fabric laminate and the ring height decreased 3 cm as a result of the ring's radial expansion. Figure 17 shows the posttest photo of the ring.

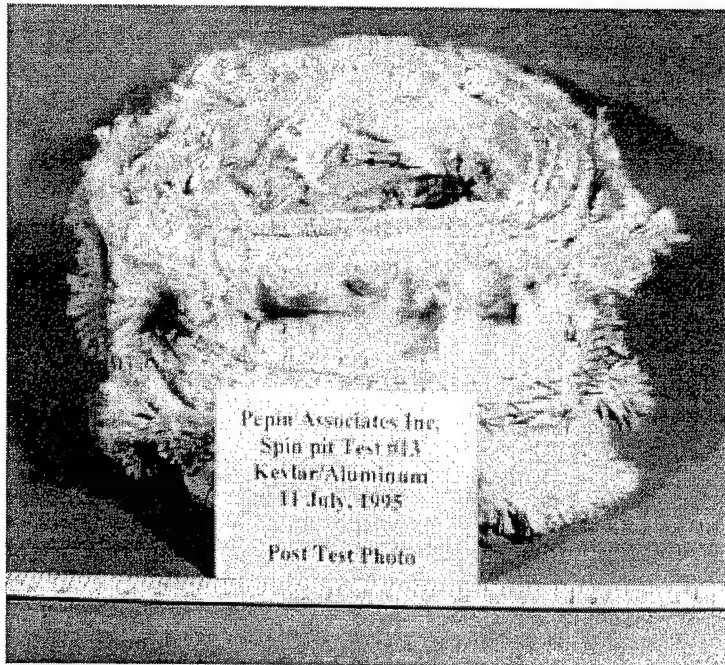


FIGURE 17. POSTTEST PHOTO OF SECOND BASELINE KEVLAR/ALUMINUM HYBRID RING

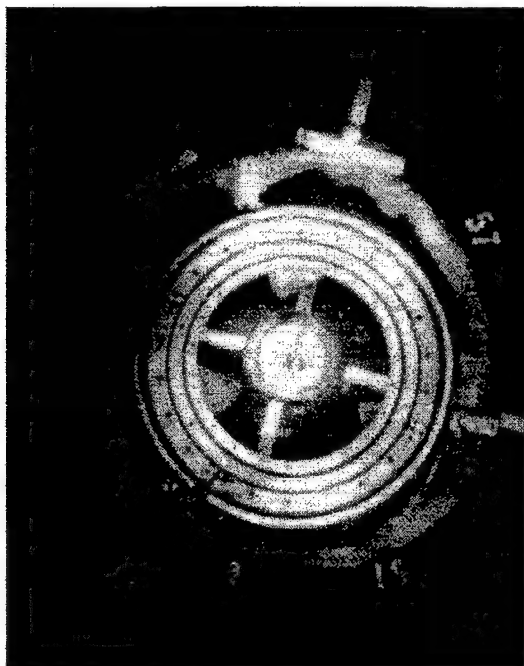
2.2.4 Large-Diameter Kevlar 29 Containment Rings.

2.2.4.1 First Large-Diameter Kevlar 29 Ring Design and Fabrication.

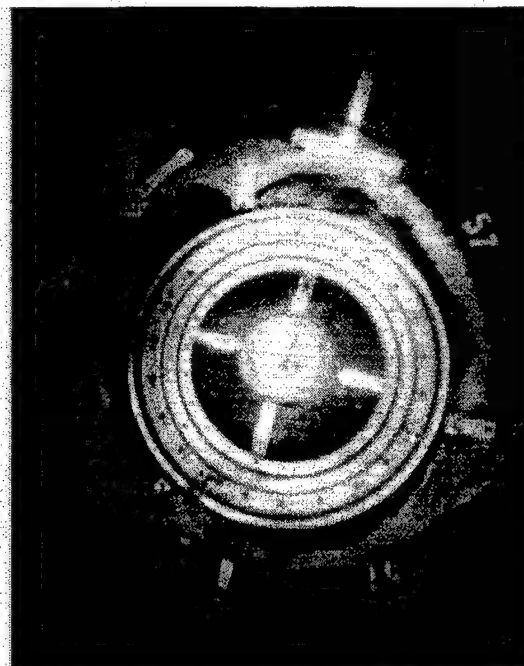
The large-diameter rings fabricated were designed to fit around the engine outer case at the plane of the second stage power turbine. Two of the spin tests were done with the T-53 combustor case mounted in the spin chamber to better simulate an actual failure. This first ring had an inside diameter of 64 cm while the axial length was the same, 22.9 cm, as that for the smaller rings. This ring was fabricated by wrapping 36 plies of the $\pm 45^\circ$ style 745 Kevlar fabric. Six of these plies have the draw strings sewn into them to create the pocket upon impact as with the small ring designs. After lay up on the mandrel, an array of aluminum rods was inserted but no facesheets were attached. This rod array had the same geometry as similar arrays on the small-diameter rings. The ring outside diameter was 71.8 cm to the fabric surface and 73.7 cm to the tips of the inserted rods. The total ring mass was 9.1 kg.

2.2.4.2 Test Results for First Large-Diameter Kevlar Containment Ring.

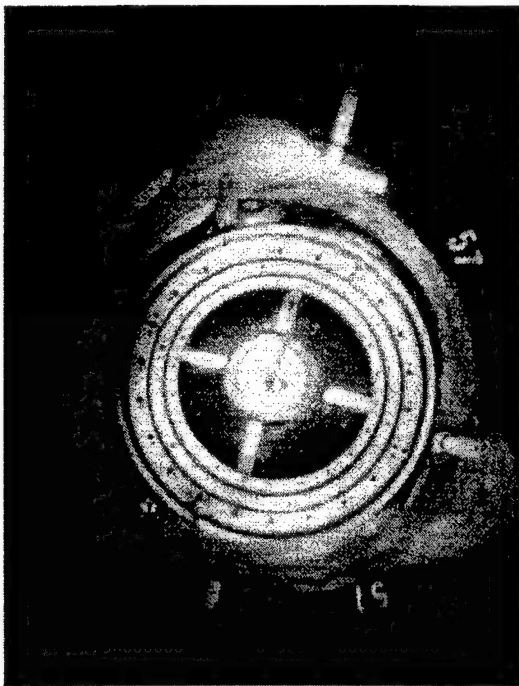
This ring was tested with the engine combustor case suspended in the spin test chamber. The containment ring completely contained the rotor burst with no penetrations of the witness ring. The trigger strip for the high-speed flash lamps was located on the containment ring ID so the first photo shows the disk fragments partially penetrated into the engine combustor case. Figure 18 shows the high-speed sequence of photographs as the disk fragments impacted the containment ring. The three disk fragments were trapped between the outer case skin and the containment ring. Figure 19 shows a close-up photo of this area.



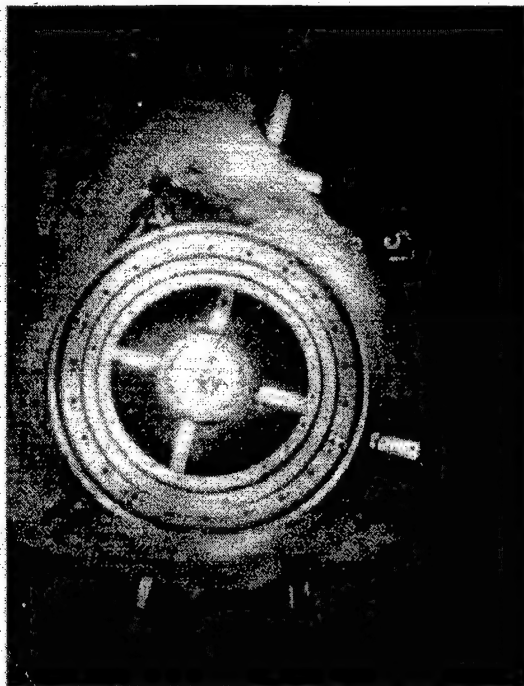
initial break of trigger strip



$t = 1.2 \text{ msec}$



$t = 2.2 \text{ msec}$



$t = 3.7 \text{ msec}$

FIGURE 18. HIGH-SPEED PHOTOS OF FIRST LARGE-DIAMETER KEVLAR
CONTAINMENT RING SPIN TEST WITH COMBUSTOR
CASE OF T-53 INSTALLED IN CHAMBER



FIGURE 19. CLOSE-UP PHOTO OF AREA BETWEEN COMBUSTOR CASE AND CONTAINMENT RING AFTER TEST OF FIRST LARGE-DIAMETER KEVLAR CONTAINMENT RING

2.2.4.3 Second Large-Diameter Kevlar Containment Ring Design and Fabrication.

The second large-diameter Kevlar containment ring was the same design as the first but with 30 plies instead of 36. Reducing the number of plies would help pinpoint the design threshold to just contain the trihub burst. The 5-cm-wide [0/90] strips were added at the edges of plies 7, 13, 19, and 25 counting from the outside diameter inward. This 30-ply ring had a mass of 7.73 kg. It also had the aluminum rod array inserted through it but no facesheets were attached. A photo of this ring is shown in figure 20. The pink foam is used as backing on the ID during manufacture. The aluminum rods were inserted from the outside surface inward through the fabric and into the foam which was initially wrapped around the internal mandrel.

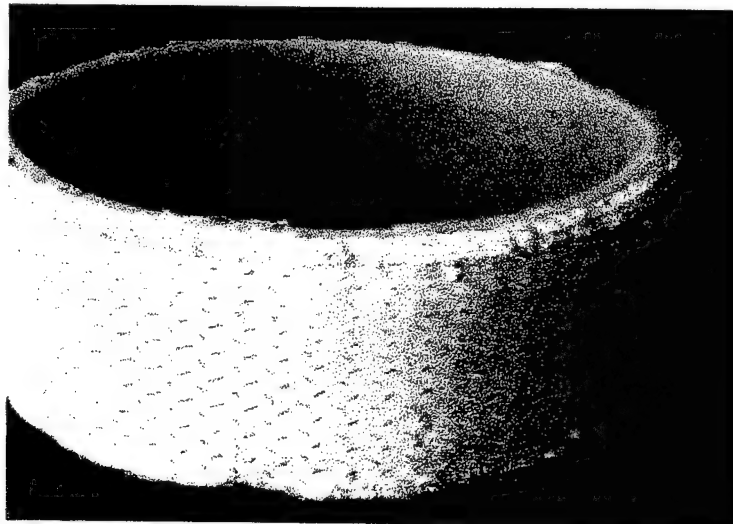


FIGURE 20. THIRTY-PLY KEVLAR CONTAINMENT RING WITH ALUMINUM RODS

2.2.4.4 Second Large-Diameter Ring Test Results.

The ring was suspended around the engine combustor case as before and the test was performed successfully. The ring contained all three disk fragments. There were two holes in the witness ring similar to those which might be caused by blade fragments. In past tests on previous programs, blades have been driven through the ring wall by a following disk segment but the disk segment itself was usually stopped. Figures 21 through 23 show posttest photos of the ring and combustor case.

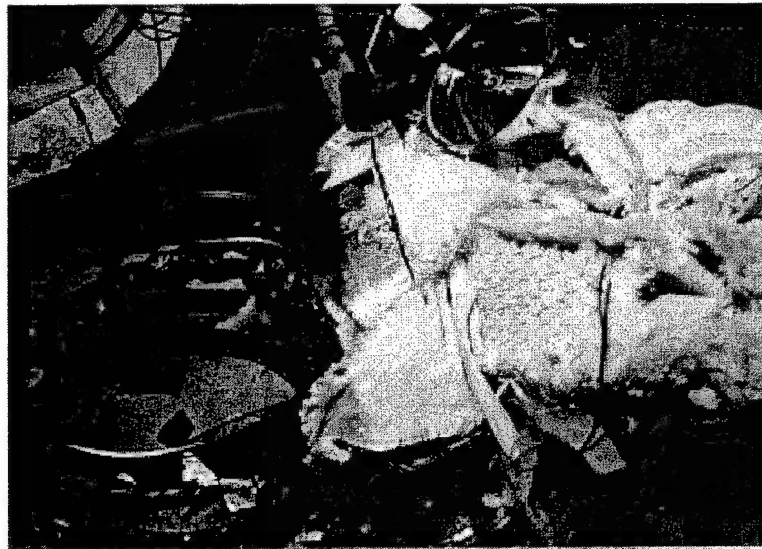


FIGURE 21. THIRTY-PLY KEVLAR CONTAINMENT RING AFTER TEST; CLOSE-UP VIEW IN CHAMBER

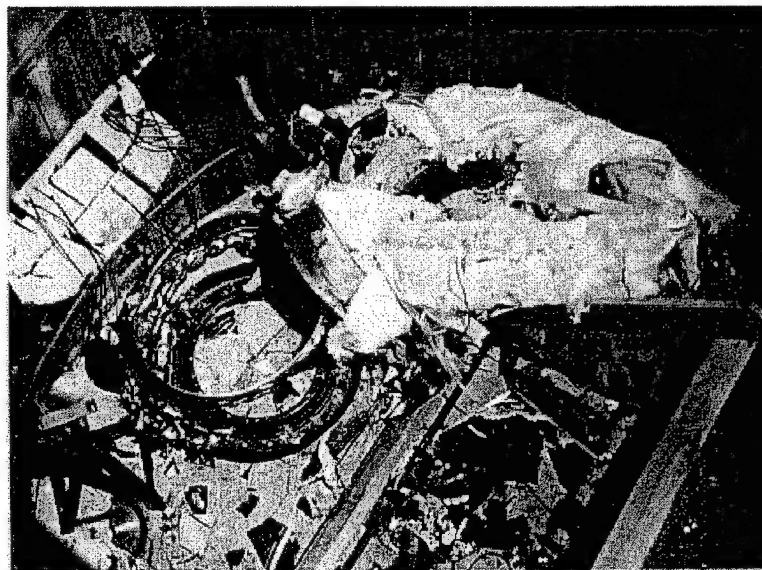


FIGURE 22. THIRTY-PLY KEVLAR CONTAINMENT RING AFTER TEST; DISTANT VIEW IN CHAMBER

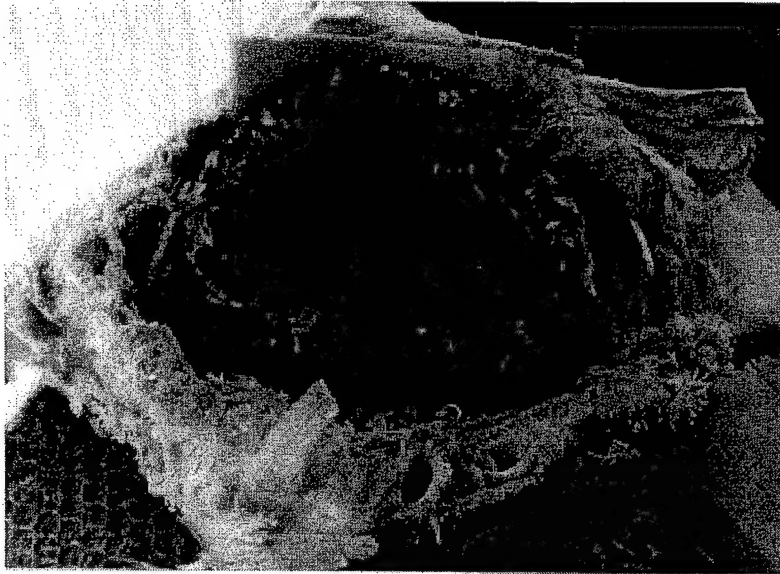


FIGURE 23. THIRTY-PLY KEVLAR CONTAINMENT RING AFTER TEST; COMBUSTOR CASE PLACED BACK INSIDE RING

2.2.4.5 Thirty-Ply Large-Diameter Kevlar Containment Ring Tested Without Engine Structure.

The test was performed to evaluate the contribution of the engine structure to containment in the previous tests. The ring design was the same as for the previous ring but this time the engine structure was not installed in the spin chamber. From the ID to the OD, this ring contained one $\pm 45^\circ$ ply, (one double ply, five $\pm 45^\circ$ plies) [7], and one $\pm 45^\circ$ ply for a total of thirty plies of the style 745 Kevlar 29 fabric. No aluminum rods were inserted into this ring. The mass of the ring was 7.3 kg (16 lb). Its ID was 67.5 cm and the axial length was the same as for the other rings. Figure 24 shows a photo of this ring before testing.

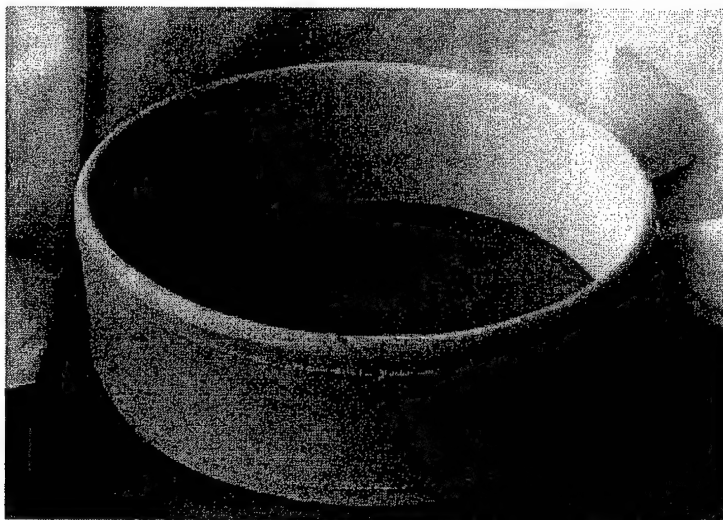


FIGURE 24. PRETEST PHOTO OF THE LARGE-DIAMETER 30-PLY KEVLAR RING TESTED WITHOUT THE ENGINE COMBUSTOR CASE

2.2.4.6 Test Results for the Large-Diameter Ring Tested Without Engine Structure.

The large-diameter ring was tested and it successfully contained all three disk fragments. The plies of the ring were significantly separated and unraveled as a result of the impacting fragments. This demonstrates the value of through-the-thickness aluminum rods as the rods tended to hold the plies together. Although a lighter-weight ring was not tested, the ring design tested is probably close to the threshold of containment. If this is so, then the engine structure does not contribute significantly to the disk fragment energy absorption; that is, the disk segments do not lose a significant amount of their energy passing through the engine structure. Figure 25 is a photo of this ring after testing.

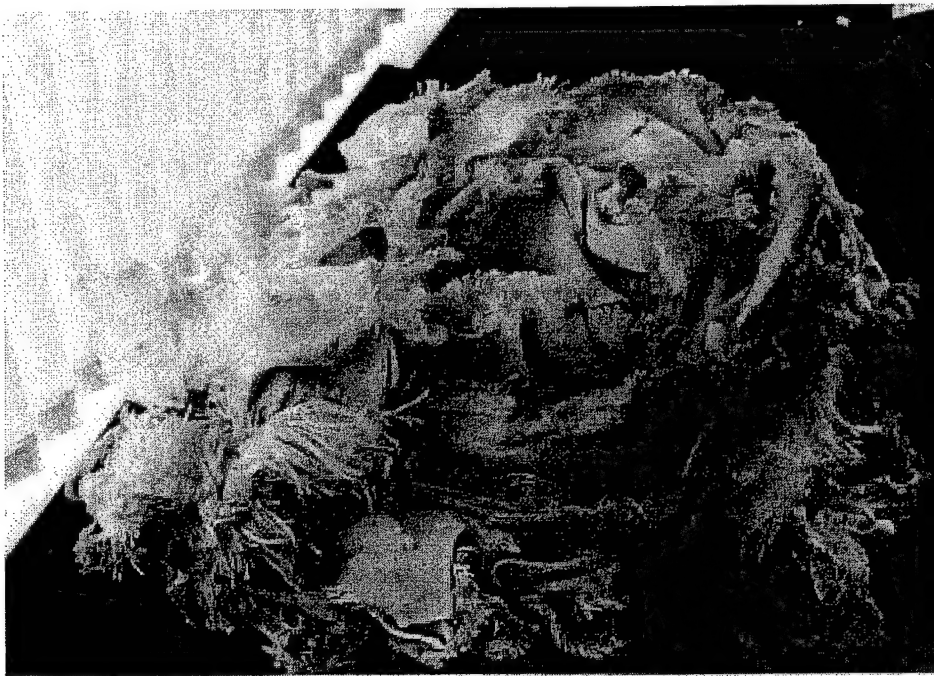


FIGURE 25. POSTTEST PHOTO OF THE LARGE-DIAMETER 30-PLY KEVLAR CONTAINMENT RING TESTED WITHOUT THE ENGINE COMBUSTOR CASE

2.2.5 Two Thermal Degradation Test Rings—Kevlar 29 and PBO.

Small-diameter Kevlar and PBO containment rings were subjected to elevated temperature for 500 hours before spin testing. As reported in a previous section both Kevlar and PBO degrade at elevated temperature but the influence of the degradation on the ability of the containment rings to stop the given rotor burst is unknown.

2.2.5.1 Small-Diameter Kevlar Thermal Test Ring.

The small-diameter Kevlar thermal test ring was designed with the same number of plies and ply orientation as the baseline ring which is known to contain the rotor burst. This is a small-diameter ring with the same 42-ply $\pm 45^\circ$ Kevlar style 745 fabric design as the baseline. The mass of the ring was 5.32 kg with no through-the-thickness rods inserted. Before the ring was

tested, it was heated in an oven to a temperature of 160°C in air for 500 hours. The degradation of Kevlar and similar fibers is a function of the time/temperature history of the fiber in service. Tests have been done at DuPont to identify the strength loss of Kevlar 29 when exposed to a given temperature over a period of time. Table 2 of section 2.1 shows that Kevlar 29 will retain 90% of its tensile strength after being exposed to 160°C air for 500 hours. Figure 26 shows the ring with imbedded thermocouples at the ID and OD. A thermocouple was also imbedded in the middle of the layup.

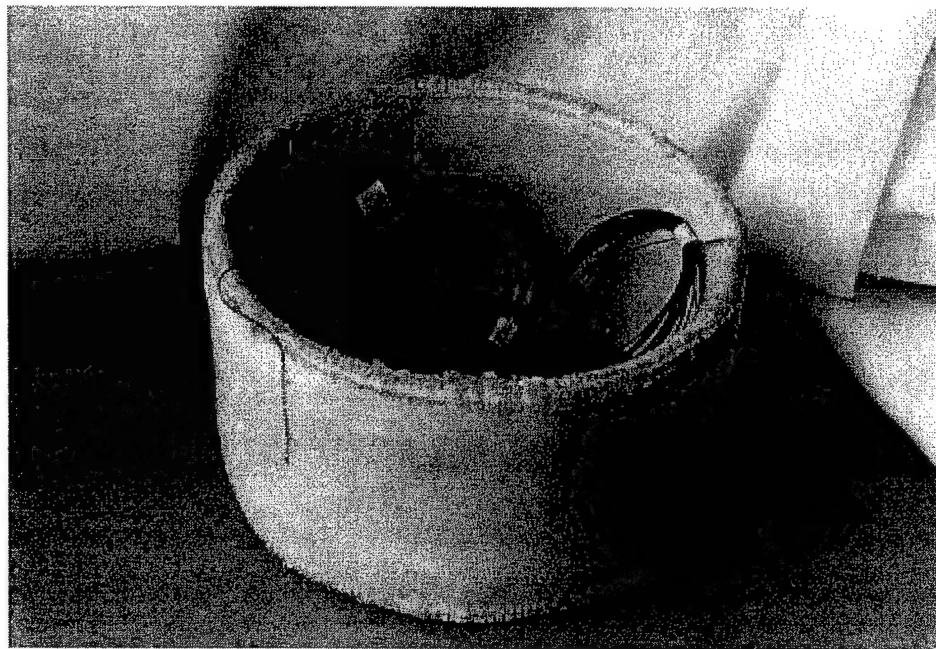


FIGURE 26. KEVLAR THERMAL TEST RING BEFORE TEMPERATURE EXPOSURE

2.2.5.2 Spin Test of Kevlar Thermal Test Ring.

After the ring was exposed to the 160°C air for 500 hours, it was then tested at the same 160°C temperature. This was done by placing a resistance heated oven inside the spin chamber to bring the ring to the required temperature before it was spin tested. Heating tapes were first used to heat the ring but they did not give adequate uniformity in temperature through the ring wall. A heat enclosure or oven was then used. Since the ring was entirely enclosed and so was not visible, high-speed photos were not taken of this test; however, high-speed photos are available for many similar tests. The temperatures of the ring during the hour before the test and at the time of the test were 171°C on the inner surface, 153°C in the middle of the ring wall, and 135°C on the outside surface.

The ring was tested and it successfully contained all three disk fragments. One of the fragments opened a hole in the ring approximately 5 cm in length. This fragment did not penetrate through the containment ring thickness. However, after losing most of the kinetic energy upon impact, the fragment dropped on the chamber floor and eventually tumbled outside the containment ring. The two other fragments were found inside the ring. The heat enclosure completely surrounded

the ring and acted as a witness shield. Two shallow dents were found in this sheet but no holes were found. Figure 27 shows the ring mounted to the spin chamber cover but the oven has not yet been placed over it. Figure 28 is a posttest photo and figure 29 shows the heating element inside the oven.

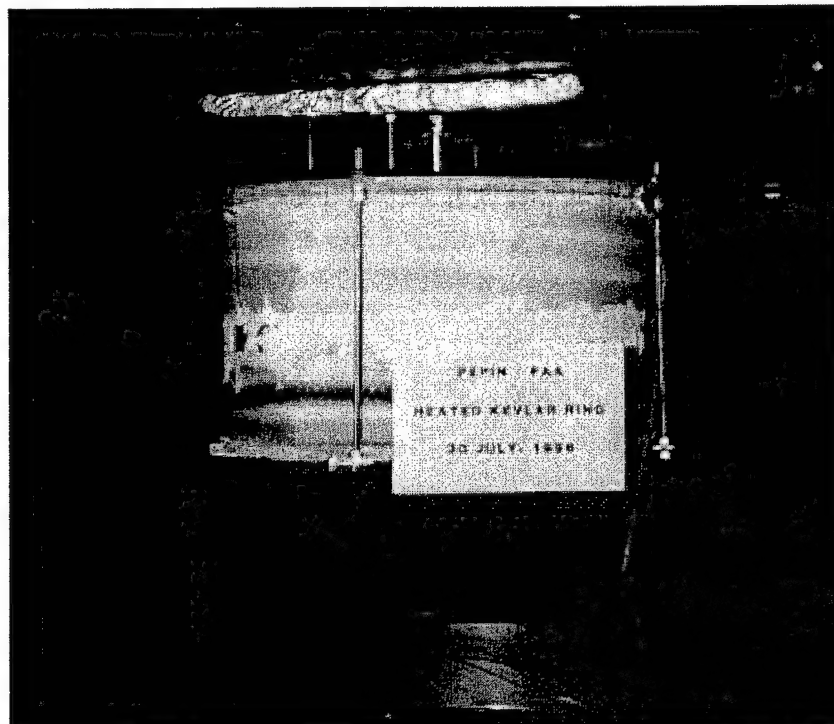


FIGURE 27. KEVLAR THERMAL TEST RING MOUNTED TO CHAMBER COVER
READY FOR TESTING



FIGURE 28. POSTTEST PHOTO OF KEVLAR THERMAL TEST RING

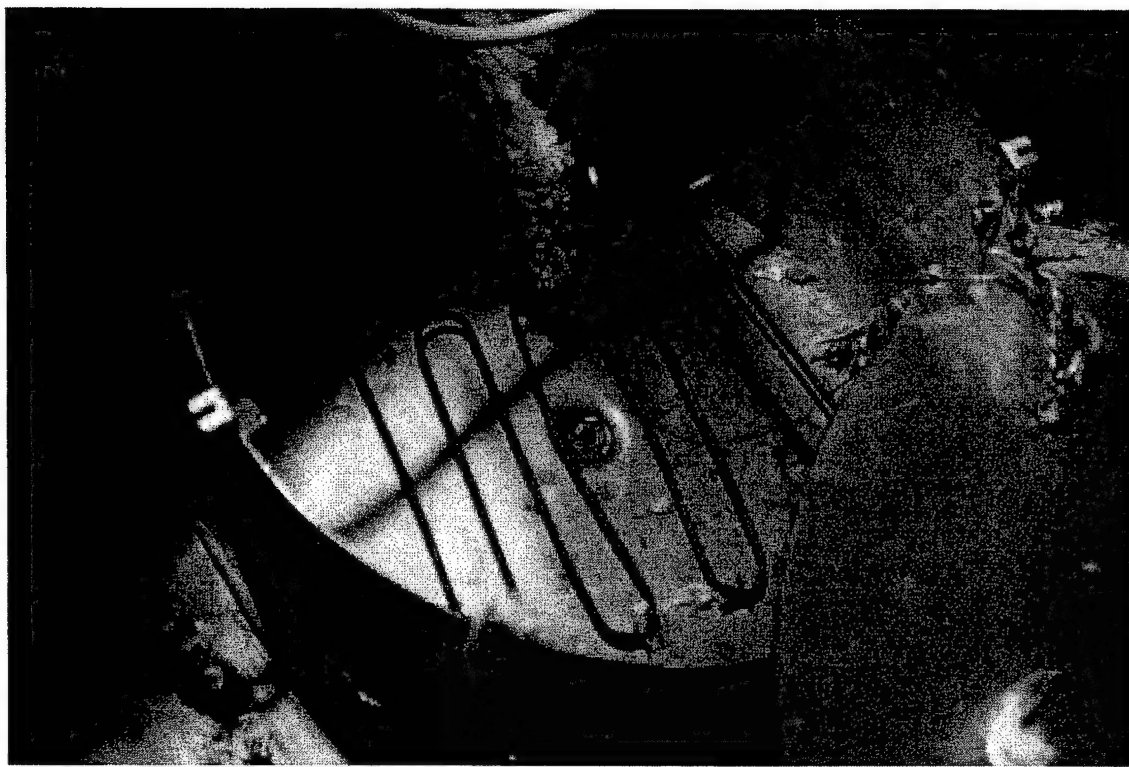


FIGURE 29. OVEN USED TO HEAT THE THERMAL TEST RINGS JUST BEFORE SPIN TESTING

2.2.5.3 Small-Diameter PBO Thermal Test Ring.

As described in section 2.1 on materials, PBO is an advanced organic fiber from Toyobo of Japan. Toyobo commercialized this fiber under the trade name Zylon™ in late 1998. In addition to its high strength, it also has good strength retention for up to 1000 hours when exposed to elevated temperatures. It starts with a much higher room temperature strength than Kevlar so the retained strength after temperature/time exposure is also much higher than Kevlar. To date no data exist beyond 1000 hrs but a small experimental program is underway at Pepin Associates, Inc. to obtain this information. Data extrapolated to 10,000 hrs show a retained tensile strength of 75% but whether this extrapolation is valid is unclear. PBO does have higher strength and temperature resistance than Kevlar so it is of interest for containment applications.

The PBO fabric used for this test ring was a 16 x 16 plain weave with 3000 denier unsized but twisted yarns. Since the tows were available only in the unsized condition, they were twisted so they could be easily woven. Fabric weight was 0.439 kg/m^2 . This ring had 43 plies with the same layup and architecture as the Kevlar thermal test ring previously described. As with the previous ring, no rods or facesheets were added. The mass of this ring was 5.73 kg and it had the following dimensions: ID 38.10 cm, OD 43.78 cm, and axial length 24.13 cm. Figures 30 through 33 show the cutting and sewing steps required to build the ring, and the finished ring is shown in figures 34 and 35.

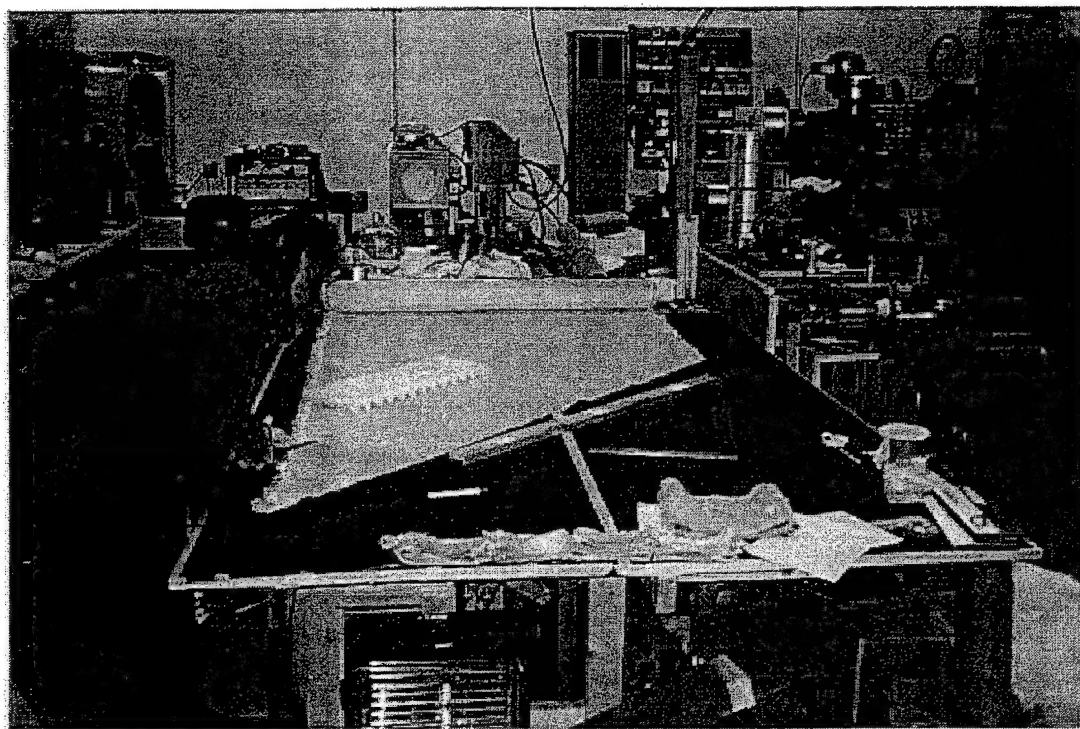


FIGURE 30. CUTTING THE PBO FABRIC AT A 45° ANGLE

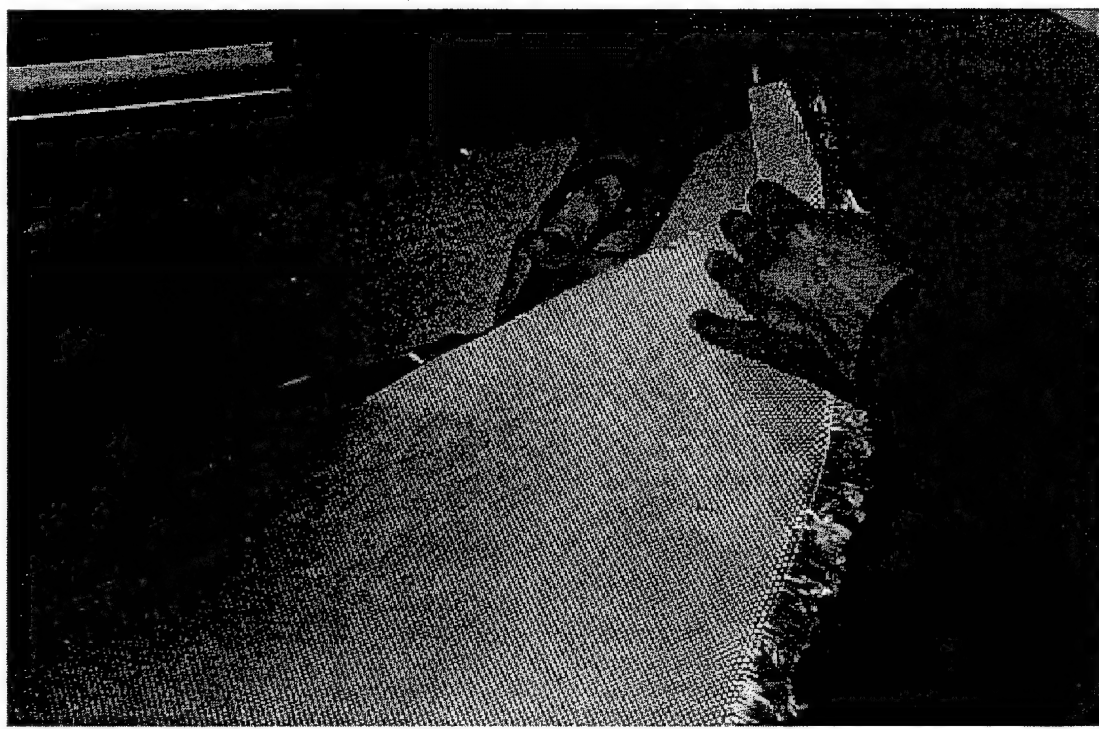


FIGURE 31. CLOSE-UP OF MANUAL CUTTING OF PBO FABRIC

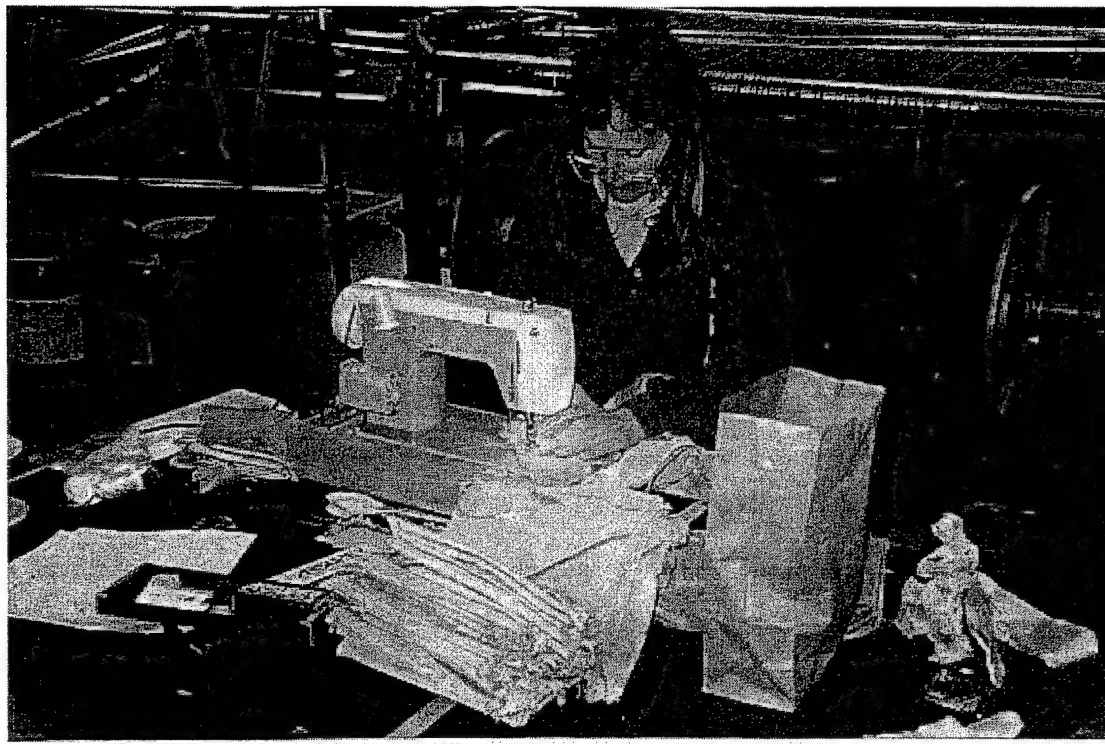


FIGURE 32. SEWING DRAW STRING STRIPS TO EDGE OF FABRIC



FIGURE 33. LAYUP OF PBO CONTAINMENT RING

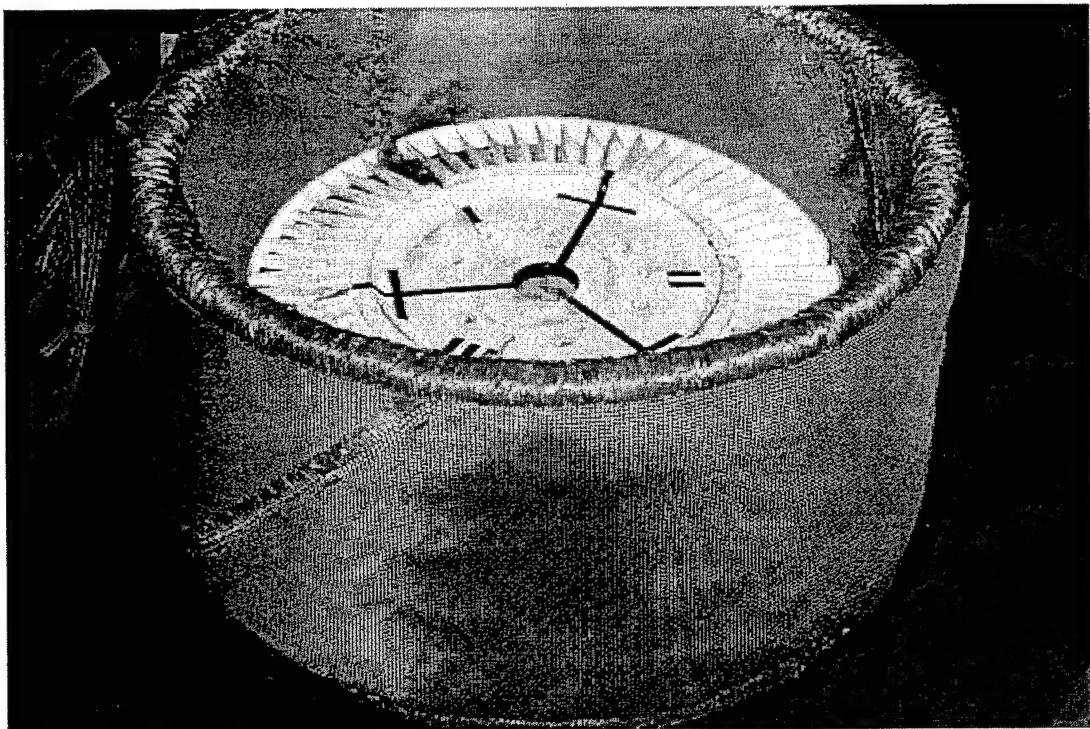


FIGURE 34. FINISHED PBO CONTAINMENT RING

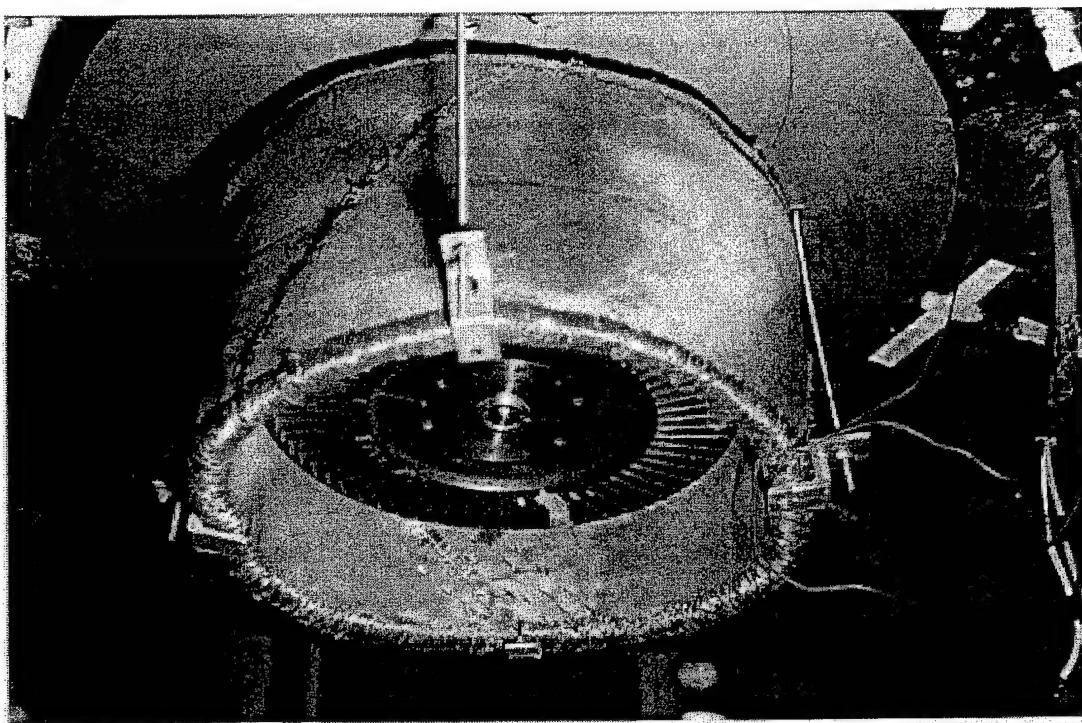


FIGURE 35. PBO CONTAINMENT RING SUSPENDED FROM COVER
OF SPIN CHAMBER

2.2.5.4 Spin Test of PBO Thermal Test Ring.

The objective of the PBO ring design was to determine the effect of temperature on the degradation of the fiber and hence its ability to contain the rotor burst after temperature exposure. The PBO ring was exposed to 200°C air for 500 hours before it was spin tested. It was then spin tested at the same 200°C temperature. Strength retention of PBO after exposure to these conditions is approximately 85%.

The rotor failed at 20,200 rpm and the ring contained all the fragments. The deepest penetration by one of the disk segments was 41 plies leaving only 2 plies undamaged. Thus, this design at the 200°C temperature was close to the threshold of containment. Figures 36 and 37 show the posttest condition of the PBO thermal test ring.



FIGURE 36. POSTTEST PHOTO SHOWING PBO RING, FRAGMENTS, AND HEATING ELEMENTS

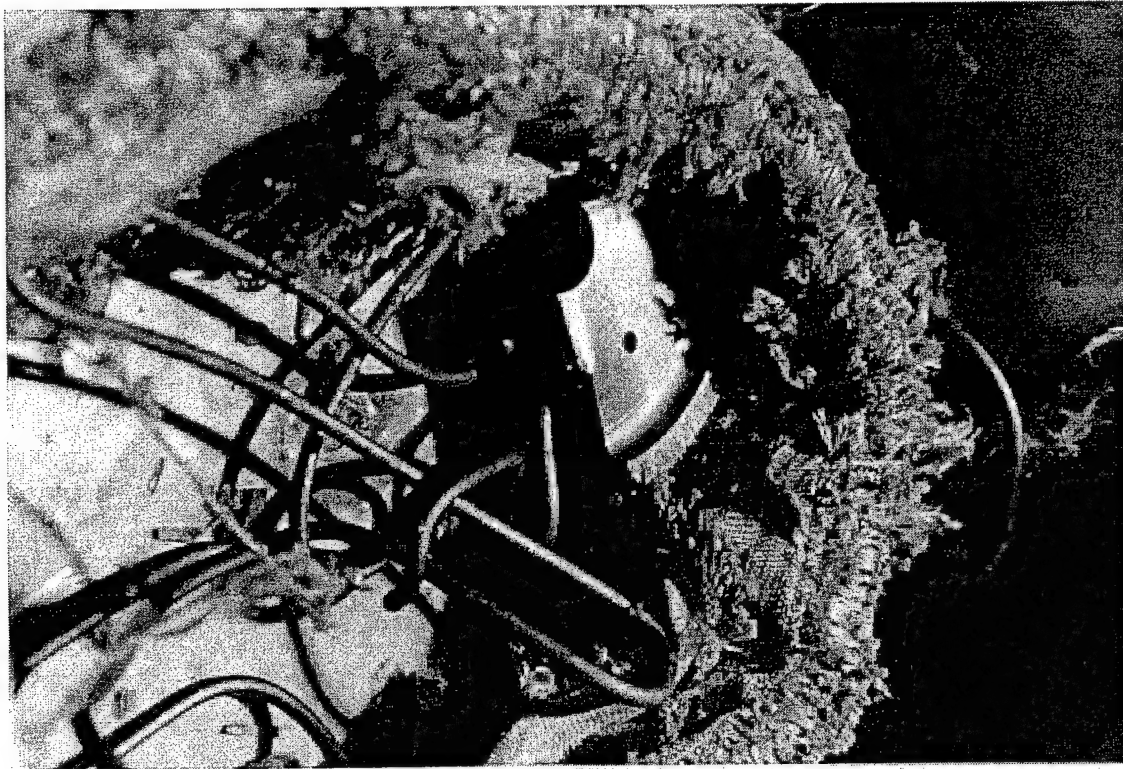


FIGURE 37. CLOSE-UP OF PBO RING AFTER TESTING

2.2.6 Full-Scale Trihub Burst Test of Containment Ring on the T-53 Engine.

2.2.6.1 Full-Scale Test Containment Ring Design and Fabrication.

The full-scale test ring was a large-diameter ring designed to fit around the T-53 engine's outer case. This ring was designed to demonstrate the ability of the hybrid panel concept to contain the rotor disk failure on a full-scale, running T-53 engine. The ring design consisted of 40 plies of Kevlar 29 style 745 with a [0/90] architecture; that is, the fiber reinforcement of the fabric coincided with the axial and circumferential directions of the containment ring. This architecture was selected to reduce the radial deformation of the containment ring since the engine was mounted to a UH1 airframe and the tail rotor shaft passes just under the engine. The 40-ply Kevlar fabric core was surrounded with a 6-4 titanium structure of through-the-thickness rods and overlaying facesheets. The rods were inserted in circumferential rows. The rods within each row were 25.4 mm apart while the rows themselves were 13 mm apart. The circumferential rows of rods alternated between + and - 45 degree rod penetration angles. The rod diameter was 1.57 mm and the nominal facesheet thickness was 0.38 mm. The rods were welded to the facesheets with a 1500-watt CO₂ laser.

The manufacturing tooling is shown in figure 38. The steel inner mandrel tooling was used to lay up the dry fabric core. A layer of aluminum foil covered the fabric layup to protect the fabric against radiant energy from welding. After the dry Kevlar fabric core has been fabricated on the mandrel, through-the-thickness rods were inserted from the inside diameter through vertical

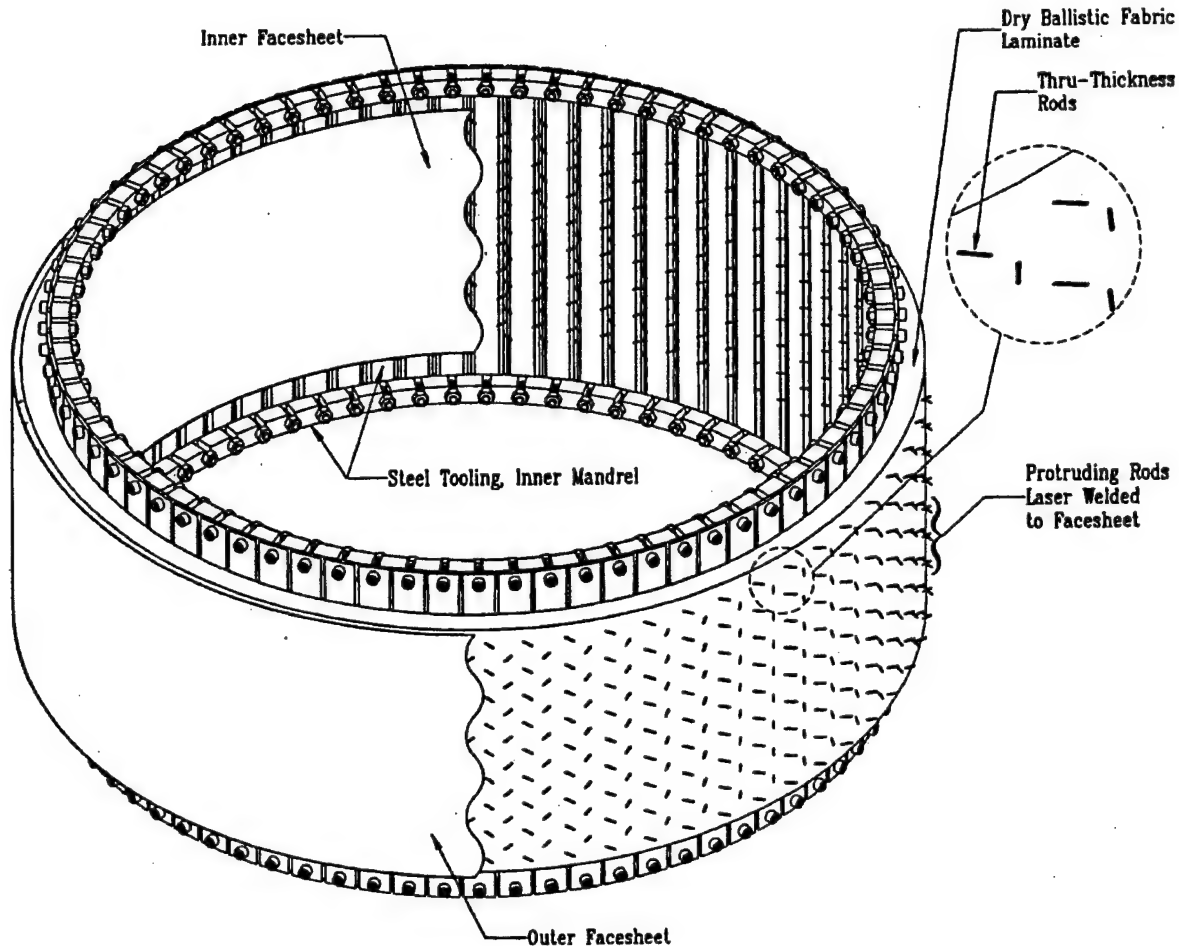


FIGURE 38. ID GRINDING OPERATION

vertical slots in the tool. This was done with a pneumatic insertion device designed and built for this task. After the rods were inserted, the protruding rods at the OD were ground so that their ends would form a cylindrical shape standing about 3.8 mm away from the foil covered fabric. Then a facesheet was wrapped around the outside surface, held with clamps, and welded to the rod ends with circumferential weld beads. The speed of welding with the laser was 700 cm/min. After the OD facesheet was attached the tooling was rearranged to hold the ring from the outside surface. The ends of the rods at the ID were then ground and the ID facesheet welded to the ends of the rods. The ID grinding operation is shown in figure 39, and the welding set up is shown in figure 40. The finished ring is given in figure 41. The final ring mass was 11.4 kg with the Kevlar comprising 9.1 kg of that total. The dimensions of the full-scale test ring were as follows: ID 63.5 cm, OD 70.6 cm, and axial length 24.8 cm.

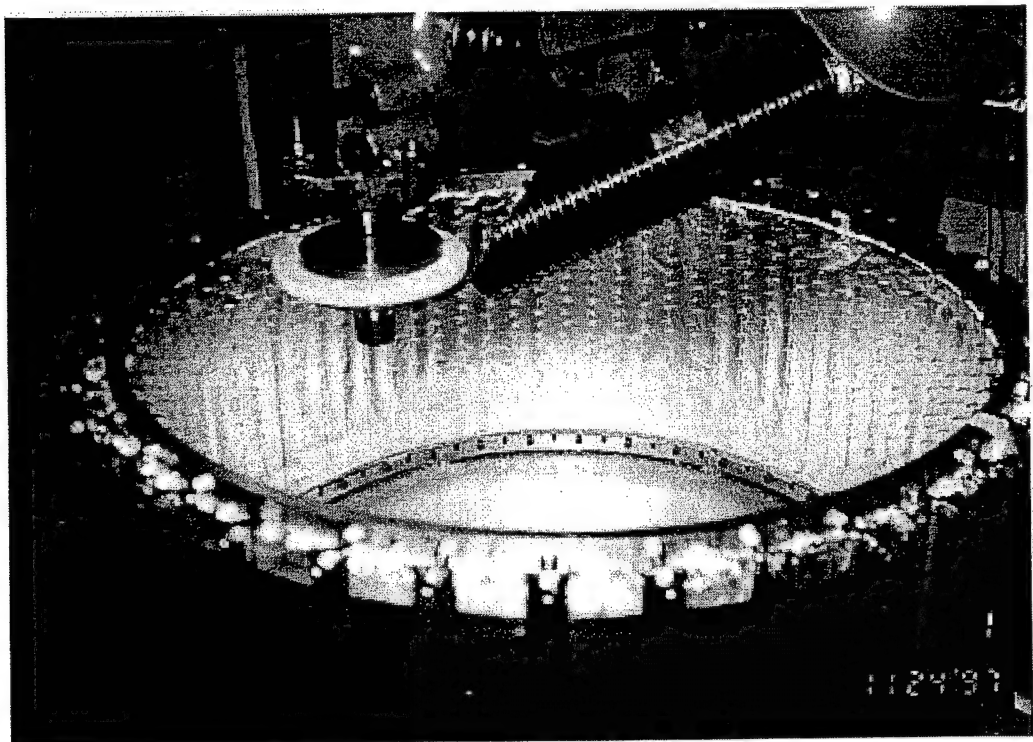


FIGURE 39. GRINDING ROD ENDS ON ID SURFACE OF FULL-SCALE TEST CONTAINMENT RING

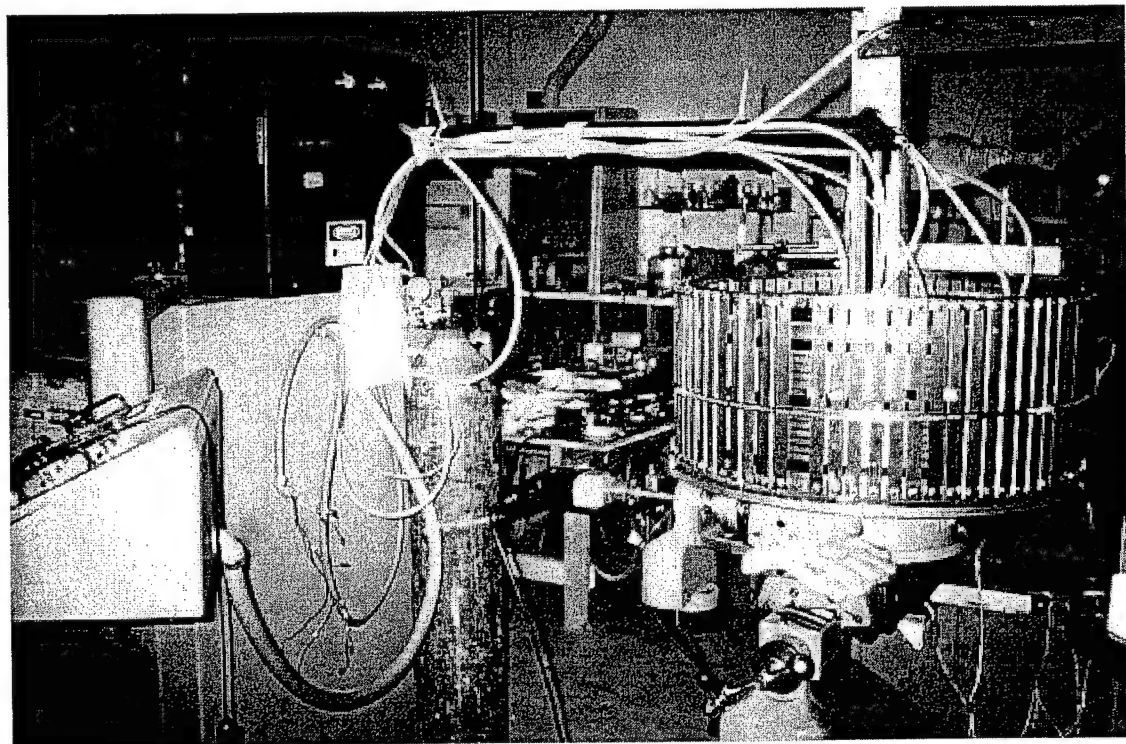


FIGURE 40. LASER SETUP FOR WELDING ID SURFACE OF FULL-SCALE TEST CONTAINMENT RING

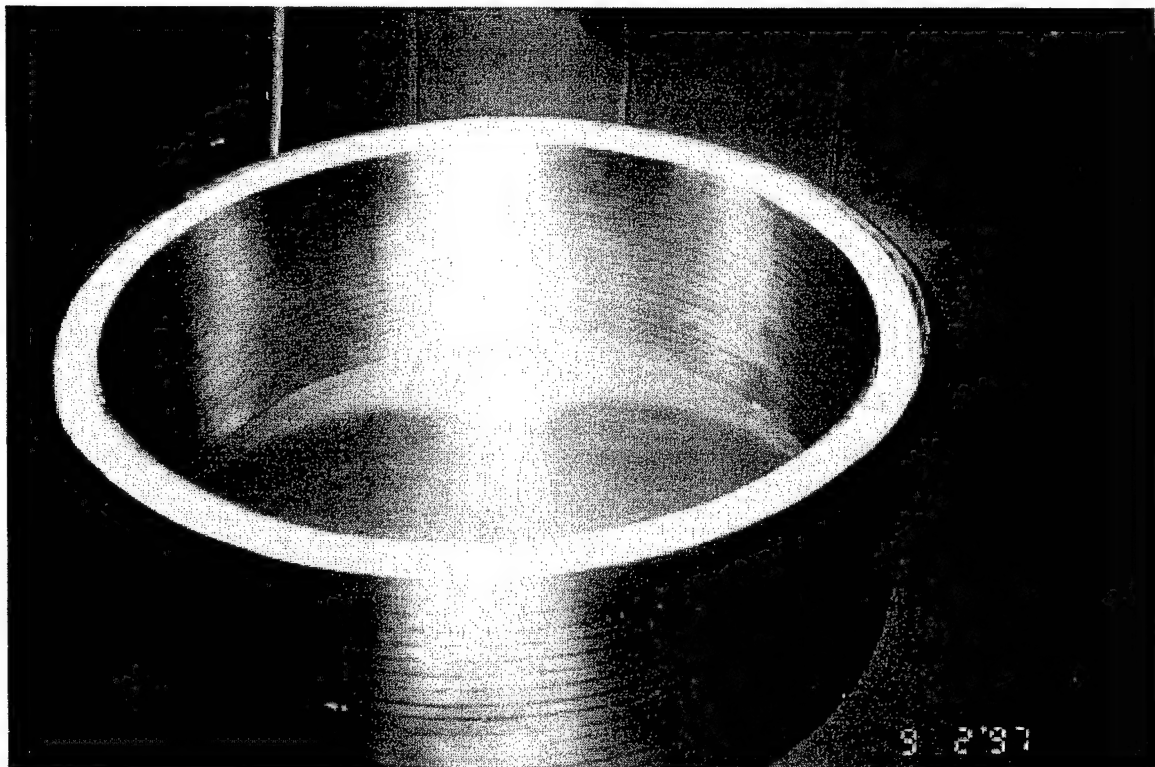


FIGURE 41. COMPLETED FULL-SCALE TEST CONTAINMENT RING

2.2.6.2 Full-Scale Test and Results.

The engine for the full-scale test was donated to this program by the U. S. Army Aviation and Missile Command in Huntsville, Alabama, (at the time the engine was donated the organization was AVSCOM in St. Louis). The T-53 engine second stage power turbine rotors which are used in the spin chamber tests have the hub area machined flat to attach to the air drive turbine shaft. The actual power turbine stage in the engine has an attached hub and shaft. It was therefore necessary to modify the disk so that the rotor would fail at the required rpm in the running engine. This modification and verification test work was done in Rotor Spin Facility (RSF) of the Naval Air Warfare Center in Trenton, New Jersey, prior to installing an actual turbine in the engine. The removal of the second power turbine from the T53 engine and the installation of the modified one were done by NAWCAD-TRN personnel at the New Jersey National Guard facility in Trenton, New Jersey. The engine was then shipped to the Naval Air Warfare Center, Weapons Division in China Lake, California, where it was mounted to a UH1 Huey helicopter for the test. Figures 42 and 43 show the engine and figure 44 shows the engine mounted on the helicopter with the containment ring attached. The midplane of the containment ring was aligned with the disk plane of the second stage power turbine.

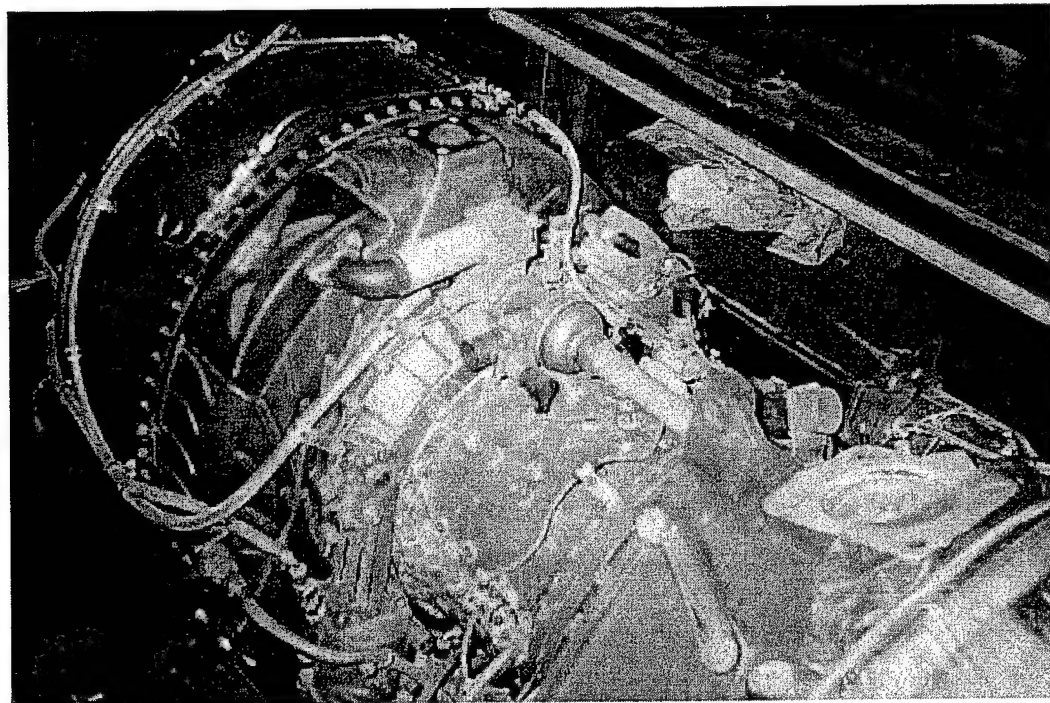


FIGURE 42. T-53 ENGINE USED IN FULL-SCALE TEST

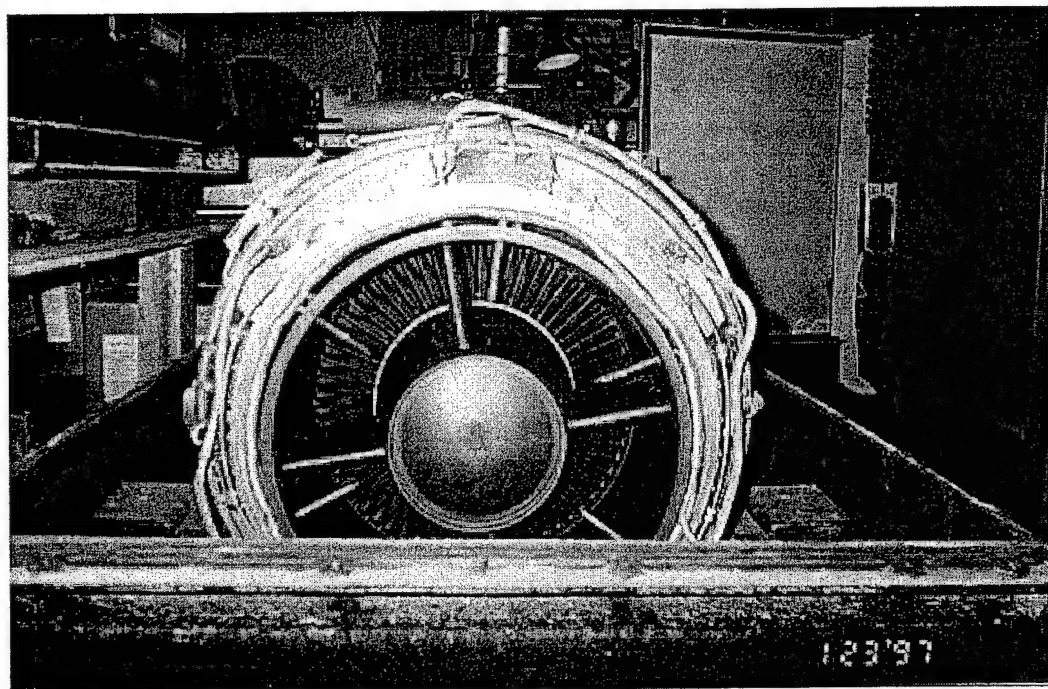


FIGURE 43. VIEW FROM THE AFT END OF THE T-53 ENGINE SHOWING THE SECOND STAGE POWER TURBINE

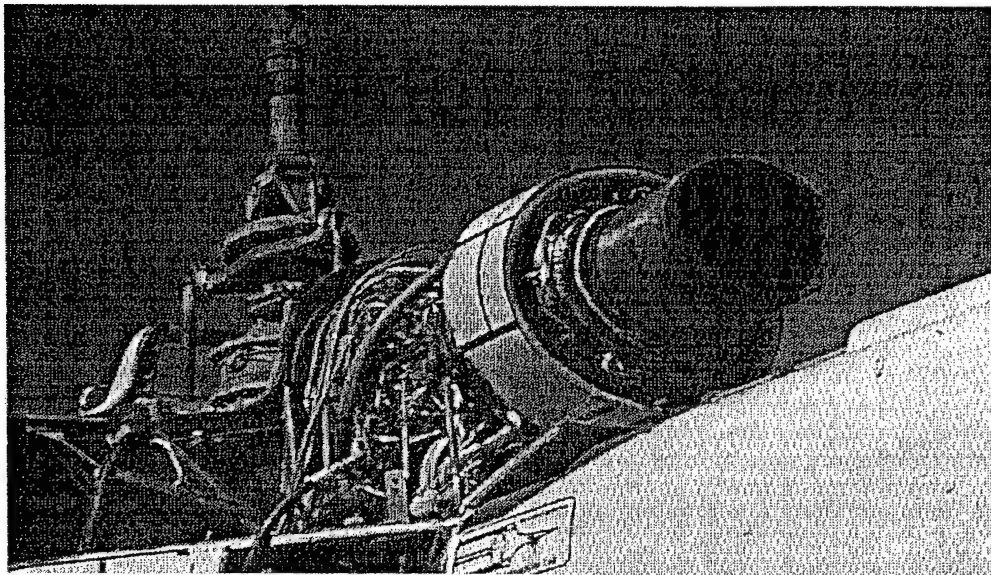


FIGURE 44. FULL-SCALE TEST SETUP SHOWING T-53 ENGINE AND CONTAINMENT RING BEFORE TEST

The full-scale engine test was performed at China Lake on September 23, 1997. The containment ring contained all three rotor disk fragments. Only a few (3-5) plies at the ID of the containment ring were penetrated indicating that the ring was probably overdesigned for the containment task; however, the radial deformation was minimized for this type of containment material and design. There was a fire of short duration and a few of the ID plies of the fabric were burned. The OD facesheet failed in tension and split along the welds while the ID facesheet failed more locally at the impact sites of the three disk fragments. The ID facesheet seemed to cover the impacting fragment thereby protecting the fabric from the sharp edges of the disk segments. The ID rod-to-facesheet welds pulled out but the rods remained in the dry laminate for the most part. Rod pull out and bending can absorb additional energy and this could be a factor in future hybrid panel designs. Both real-time and high-speed video were taken from four camera positions around the helicopter. Figures 45 through 48 show posttest photos from different angles around the helicopter.

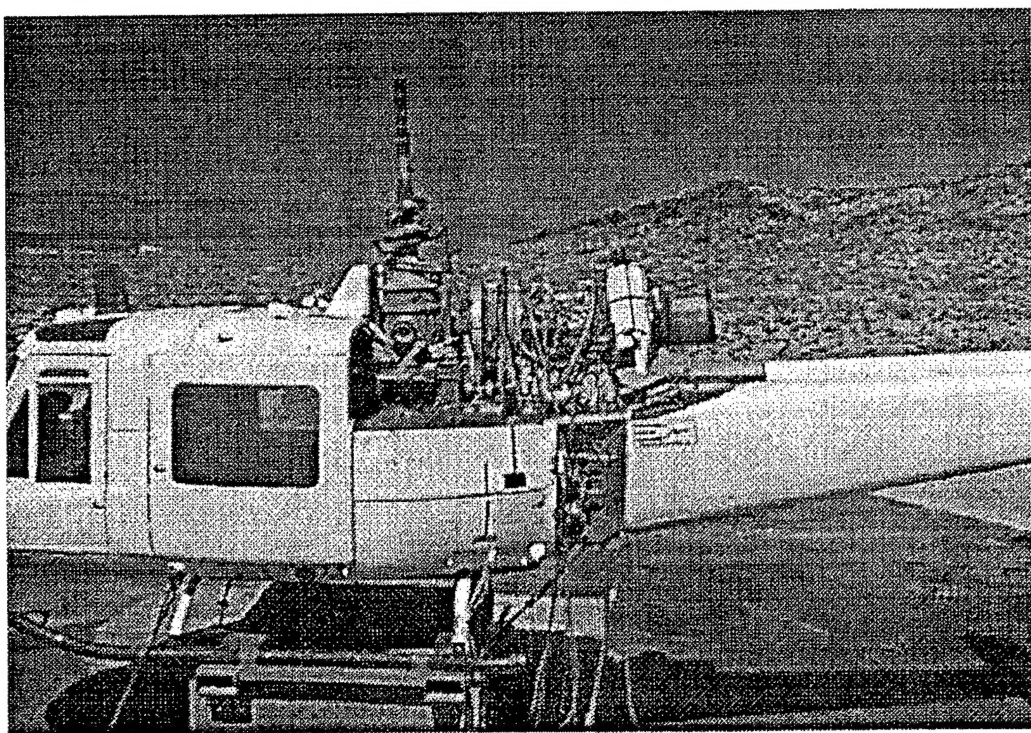


FIGURE 45. POSTTEST PHOTO SHOWING HELICOPTER AIRFRAME,
ENGINE, AND CONTAINMENT RING

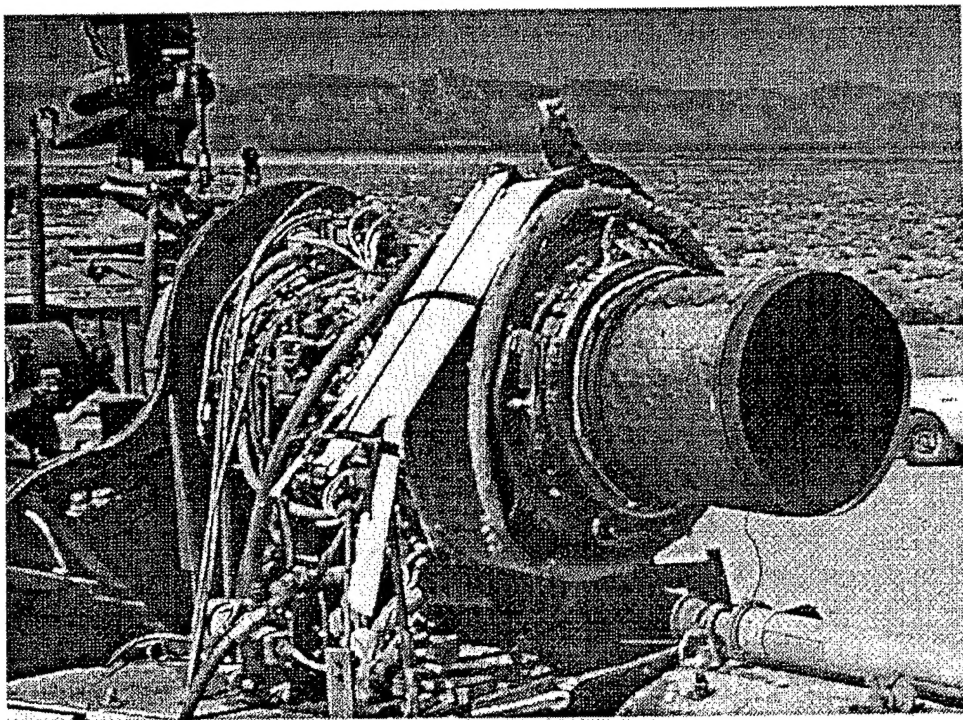


FIGURE 46. CLOSE-UP OF THE LEFT SIDE OF THE ENGINE SHOWS OUTER
FACESHEET PEELED BACK

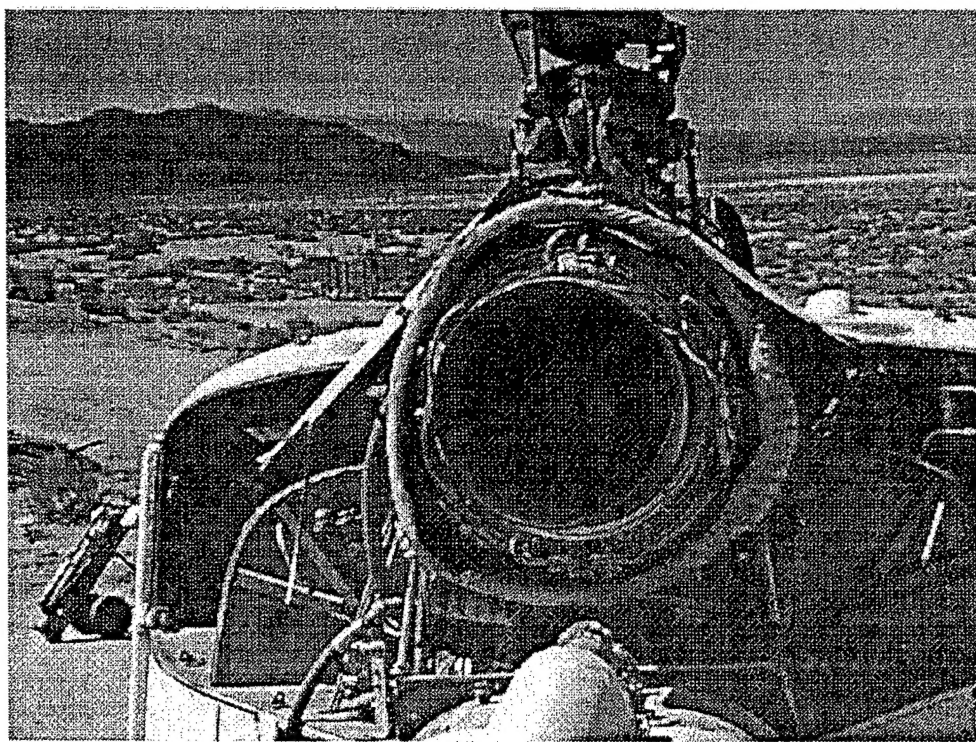


FIGURE 47. VIEW FROM THE TAILPIPE; BULGES IN THE RING INDICATE DISK
FRAGMENT IMPACT

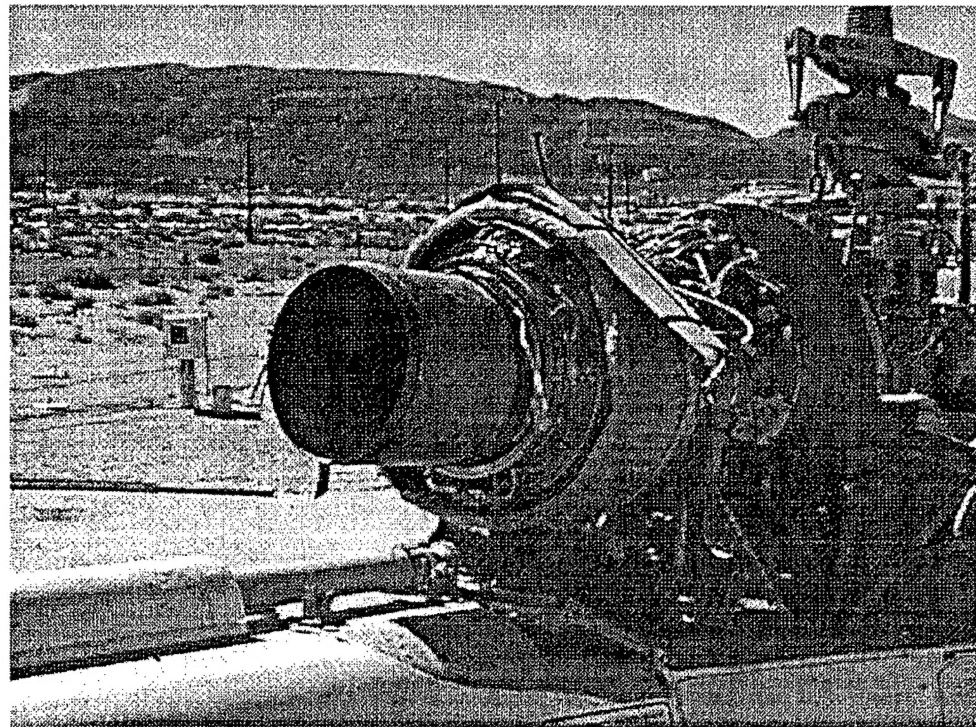


FIGURE 48. POSTTEST VIEW FROM THE RIGHT SIDE OF THE ENGINE

The following table summarizes the results of the entire test program.

TABLE 3. CONTAINMENT RING DESIGN AND TEST SUMMARY

Ring Number	Test Date	Ring Design	Mass, kg	Contained?
I	3/9/95	S glass baseline, with Teflon interleaves, [0/90] orientation	9.64	no
II	7/12/95	Polyimide coated S glass ring, [0/90]	13.60	no
III	8/2/95	S glass, 250 roving, $\pm 45^\circ$ orientation	13.60	no
IV	3/8/95	Kevlar 29 style 745; 42 plies $\pm 45^\circ$ /hybrid	7.14	yes, multiple fragments
V	7/11/95	Same as IV with foam under facesheets	8.81	yes
VI	10/4/95	Kevlar 36 ply $\pm 45^\circ$ /tested with combustor	9.10	yes
VII	3/1/96	Kevlar 30 ply $\pm 45^\circ$ /tested with combustor	7.73	yes
VIII	4/3/96	Kevlar 30 ply $\pm 45^\circ$ /tested without structure	7.3	yes
IX	7/29/96	Kevlar 42-ply small-diameter thermal test 160°C	5.32	yes
X	3/3/97	PBO 43-ply small-diameter thermal test 200°C	5.73	yes
XI	9/23/97	Full-scale test, 20-ply Kevlar/titanium	11.40	yes

3. CONCLUSIONS.

The current fabrication, development, and test program was based on using ballistic fabric in combination with, in some tests, a metallic surrounding structure to absorb the energy of a turbine rotor disk failure. The following conclusions have been drawn from these results:

- Based on this test program, dry, unimpregnated S glass may not be an effective material to absorb the energy of high-speed fragments.
- Kevlar 29 is a good baseline ballistic fabric for containment structures. It remains effective after exposure to 160°C air for 500 hours.
- PBO is an effective, lightweight, energy-absorbing material for containment structures. Tests have shown that it is effective at room temperature and after exposure to 200°C air for 500 hours.
- Off-axis fabric reinforcement in a containment ring yields a lighter-weight ring to stop a given energy level but the deformation of the ring is greater than that of the [0/90] reinforcement orientation.
- A hybrid panel structure can perform the dual role of supporting static/dynamic loading as well as absorbing the energy of high-velocity fragments with a minimum of weight and enclosed volume.

- f. Fabric-based containment structures expand radially as the impacting fragments are slowed and their energy is absorbed by the structure. If a large mass is present in this expansion zone, then the containment structure can be pinched between this mass and the impacting fragment. This condition can cause shear failure of the energy-absorbing fabric and this type of failure usually creates a hole through which fragments may escape.
- g. A hybrid structural/energy-absorbing panel or ring can be fabricated using titanium rods and facesheets. The joints can be welded with a CO₂ laser. The small heat affected zone of the weld does not warp even a thin facesheet. The ballistic fabric can be protected by foil and is not damaged by the nearby welding.

4. REFERENCES.

1. Pepin, J. N., "Fiber-Reinforced Structures for Turbine Engine Fragment Containment," AIAA paper 93-1816 presented at the AIAA/SAE/ASME/ASEE 29th Joint Propulsion Conference and Exhibit, Monterey, California, June 28-30, 1993.
2. FAA Advisory Circular Draft, "Design Precautions for Minimizing Hazards to Aircraft From Uncontained Turbine Engine and Auxiliary Power Unit Rotor Failures," AC 20-128x, June 21, 1991.
3. "Report on Aircraft Engine Containment," Society of Automotive Engineers, Inc. Aerospace Information Report AIR 4003, September 1987
4. Kuroki, T., Tanaka, Y., Hokudoh, T., and Yabuki, K., "Heat Resistance Properties of Poly(p-phenylene-2,6-benzobisoxazole) Fiber," *J. Appl. Polym. Sci.* 65:1031-1036, 1997.
5. Pereira, J. M., Roberts, G. D., and Revilock, D. M., "Elevated Temperature Ballistic Impact Testing of PBO and Kevlar Fabrics for Application in Supersonic Jet Engine Fan Containment Systems," NASA Technical Memorandum, November 1997.
6. Le, D. D., "Evaluation of Lightweight Material Concepts for Aircraft Turbine Engine Rotor Failure Protection," DOT/FAA/AR-96/110, July 1997.
7. Private communication, Greg Harville, Bell 222 Captain, New Hampshire Helicopters, April 1989.